

1 Supplementary information for:  
2 **Endophytic and ectomycorrhizal, an overlooked dual ecological niche? Insights from natural**  
3 **environments and *Russula* species.**

4  
5 **Authors:**  
6 Liam LAURENT-WEBB<sup>1\*</sup>, Philippe RECH<sup>1</sup>, Amélia BOURCERET<sup>1</sup>, Chloé CHAUMETON<sup>2</sup>, Aurélie  
7 DEVEAU<sup>3</sup>, Laurent GENOLA<sup>4</sup>, Mélanie JANUARIO<sup>1</sup>, Rémi PETROLLI<sup>1</sup>, Marc-André SELOSSE<sup>1,5,6\*</sup>

8 <sup>1</sup> Institut de Systématique, Évolution, Biodiversité (ISYEB), Muséum national d'Histoire naturelle,  
9 CNRS, Sorbonne Université, EPHE, UA, 57 rue Cuvier, 75005 Paris, France.

10 <sup>2</sup> Sorbonne Université, Institute of Biology Paris-Seine, Paris 75005, France.

11 <sup>3</sup> UMR IAM, Université de Lorraine, INRAE, 54280, Champenoux, France.

12 <sup>4</sup> Station Trufficole du Montant, EPLEFPA Cahors-LeMontat, 422 Lacoste, 46090, Le Montat.

13 <sup>5</sup> Faculty of Biology, University of Gdańsk, ul. Wita Stwosza 59, 80-308 Gdańsk, Poland.

14 <sup>6</sup> Institut Universitaire de France.

15

16 **\* Corresponding authors:**

17 Liam LAURENT-WEBB ([liam.laurent@cirad.fr](mailto:liam.laurent@cirad.fr); ORCID: 0000-0003-1156-6432)

18 Marc-André SELOSSE ([ma.selosse@wanadoo.fr](mailto:ma.selosse@wanadoo.fr); ORCID: 0000-0003-3471-9067)

19

20 **Other authors information (e-mail; ORCID):**

21 Amélia BOURCERET: [amelia.bourceret@mnhn.fr](mailto:amelia.bourceret@mnhn.fr)

22 Chloé CHAUMETON: [chloe.chaumenton@sorbonne-universite.fr](mailto:chloe.chaumenton@sorbonne-universite.fr); 0009-0005-7926-3261

23 Aurélie DEVEAU: [aurelie.deveau@inrae.fr](mailto:aurelie.deveau@inrae.fr); 0000-0001-6266-5241

24 Laurent GENOLA: [laurent.genola08@gmail.com](mailto:laurent.genola08@gmail.com)

25 Mélanie JANUARIO: [melanie.januario@mnhn.fr](mailto:melanie.januario@mnhn.fr)

26 Rémi PETROLLI: [remi.petrolli@mnhn.fr](mailto:remi.petrolli@mnhn.fr)

27 Philippe RECH: [philippe.rech@mnhn.fr](mailto:philippe.rech@mnhn.fr); 0000-0002-6631-9888

28

29 **Key words:** ectomycorrhizae, endophytes, *Russula*, metabarcoding, FISH microscopy

30 **Supplementary methods (1-4).....** **2**

31 **Supplementary discussions (1-2).....** **13**

32 **Supplementary tables (1-7).....** **16**

33 **Supplementary figures (1-10).....** **22**

34 **References .....** **33**

35

36 **Supplementary Methods (1-4)**

37

38 **Supplementary Methods 1: Study sites and sampling**

39

40 This study encompasses results from nine sampling sites presented below (Fig. S1; Table S1).

41

42 **Methods S1.1: Endophytism of EcM fungi in non-EcM plant species in several sites across France**

43 We sampled non-EcM plant individuals in three forest sites (F1, F2 and F3) and one meadow (M1)  
44 across France in order to test whether the dual endophyte/EcM niche is a common feature observed  
45 in sites separated by 20 to 450km (Fig. S1). These samples were collected between May 2016 and April  
46 2019 in four locations (Table S1). We sampled roots of non-EcM plants in two forests characterized by  
47 an acidic soil dominated by chestnut trees (*Castanea sativa*; F1 and F2 sites). At both sites, the four  
48 most abundant herbaceous species were selected and several individuals were sampled (Table S1).  
49 Four root tips per individual were pooled. We additionally collected rhizospheric soil in order to  
50 characterize a potential root filter on rhizosphere EcM fungi. Rhizospheric soil of each individual was  
51 collected by gently shaking the soil closely attached to roots. Root samples of the F3 site were collected  
52 on a calcareous field in Corrèze, near but outside a productive *Tuber melanosporum* orchard. M1  
53 samples were collected in a meadow in a closed botanical garden of the National Museum of Natural  
54 History in Paris and 4 root tips per non-EcM plant individual were collected and treated individually  
55 (i.e., no pooling). All collected root tips (F1, F2, F3 and M1 sites) were selected based on their apparent  
56 good health and checked for the absence of ectomycorrhizae (especially root tips of ligneous species).  
57 They were surface sterilized as follows: root tips were washed three time in 70% ethanol (3x5min) and  
58 in 0.9% bleach. They were then rinsed three times in sterile water and stored at -20°C before molecular  
59 analysis.

60

61 **Methods S1.2: Detection of EcM fungi in roots of non-EcM plants by amplicon sequencing and**  
62 **fluorescence in situ hybridization in Gaillac sites**

63 In order to investigate the variability of the dual EcM/endophyte niche at smaller scale, we sampled  
64 roots from non-EcM plants species in 5 sites near Gaillac in South-West of France, distant from 10 to  
65 800m. The sites are characterized by a calcareous soil. We collected samples in (i) two forests  
66 dominated by oaks, where fruitbodies of *Russula* spp. and other EcM fungi have been observed (F4  
67 and F5), (ii) a meadow where no fruitbodies were observed (M2), and (iii) areas at the edge of the  
68 forests with only non-EcM plant species but producing a large number *Russula* spp. fruitbodies (MF1  
69 and MF2; Fig. S1; Table S1).

70 Samples were collected at different times: in June 2021, we collected roots only for amplicon  
71 sequencing (**Methods S2**) in the five sites (MF1, MF2, F3, F5 and M2). The sampling was representative  
72 of the plant community within each site, and therefore varied between them. We sampled individuals  
73 of the same species in the different sites whenever possible. For each plant individual, three root tips  
74 were collected, carefully washed in sterile Mili-Q water, pooled and kept dried in silica-gel. Samples  
75 were kept dry until molecular work. We also collected *Russula* spp. fruitbodies in the forest edge site  
76 MF1 for molecular identification and fluorescence *in situ* hybridization probe design (see **Methods S4.1**  
77 for probe design). In September 2021, we collected plant individuals for both amplicon sequencing and  
78 fluorescent *in situ* hybridization (*FISH*) microscopy in both edges sites (MF1 and MF2). We carefully  
79 dug up individuals in order to keep the roots in their surrounding soil. Samples were kept at 4°C in  
80 individual zip-locks. The next day in the laboratory, we removed the rhizospheric soil and selected  
81 three root tips per individual. Each root tip was cut in two pieces: one piece was carefully washed in  
82 sterile water, flash-frozen in nitrogen and kept at -20°C before molecular analysis. The other half was  
83 washed in PBS 1% and fixed in PFA 4% to fix RNAs overnight at 4°C before *FISH* and microscopy  
84 observations (**Methods S4**). Fixed samples were kept at -20°C before hybridization. In September 2021,  
85 one *Russula* sp. fruitbodie was also collected and processed for *FISH* in order to test our newly designed  
86 probes (see **Methods S4**). Finally, we sampled individuals of two plant species (*Ranunculus bulbosus*  
87 and *Pilosella officinarum*) for *FISH* in July 2023 and processed them as described above.

88 **Supplementary Methods 2: Sequencing of fruitbodies and amplicon sequencing of**  
89 **root/rhizospheric fungal communities**

90

91 **Methods S2.1: Fruitbodies gDNA extraction and 18S/ITS2 rRNA PCR**

92 We sequenced the 18S and ITS region of the ribosomal operon of *Russula* spp. fruitbodies harvested  
93 in Gaillac sites to design fluorescence *in situ* hybridization probes (18S) and for taxonomic identification  
94 (ITS). 20 to 80 mg of dried (in silica-gel) fruitbodies were used to extract gDNA. Samples were  
95 mechanically disrupted 3 times at 30 hz in a TissueLyser II (Qiagen, USA) during 30 sec with 2 grinding  
96 steel balls (Retsch, Luxembourg). gDNA was extracted using the commercial DNeasy Plant Mini kit  
97 (Qiagen, USA) according to the manufacturer's instructions, and eluted in 100 $\mu$ l of TE buffer. Extracted  
98 gDNA was quantified using Qubit™ fluorometer (Life Technologies, Singapore) and Qubit™ (1X dsDNA  
99 High Sensitivity Assay Kit, Invitrogen). 18S rDNA was amplified from each fungal gDNA extraction by  
100 PCR using the universal fungal primers NS1 (3'-GTAGTCATATGCTTGTCTC-5') and NS8 (3'-  
101 TCCGCAGGTTCACCTACCGA-5'; White *et al.*, 1990). The ITS1-5.8S-ITS2 rDNA region was amplified using  
102 primers ITS5 (3'-GGAAGTAAAAGTCGTAACAAGG-5') and ITS4 (3'- TCCTCCGCTTATTGATATGC-5'; White  
103 *et al.*, 1990). PCR reaction was performed by mixing 3ng of gDNA, 7.5pmole of each primer, 2U DFS-  
104 Taq DNA Polymerase (Bioron Life Science, Germany), 75 $\mu$ g Bovine Serum Albumin (Sigma, USA),  
105 200 $\mu$ M of each dNTP (New England Biolabs), and 1x Incomplete NH4 (Bioron Life Science, Germany).  
106 The optimal conditions for PCR amplification of 18S rDNA segments with these primers were 95°C  
107 10min, followed by 30 cycles at 95°C 30 sec, 53°C 30 sec, 72°C 2 min, and a final elongation step at  
108 72°C 10 min. The PCR products were subjected to Sanger sequencing from both directions using the  
109 same set of primers (Eurofins Genomics, Germany). Additionally, a couple of internal primers were  
110 designed specifically on conserved regions with the free software Primer3 (Untergasser *et al.*, 2012)  
111 to sequence the extremities of each 18S PCR fragments. The obtained electropherograms were  
112 checked, sequences were corrected and submitted to GenBank under the accession number  
113 OR910623-OR910639. ITS sequences taxonomy was assigned against the UNITE online database using  
114 BLAST tool (<https://unite.ut.ee/analysis.php#>).

115

116 **Methods S2.2: Amplicon sequencing of the fungal communities**

117 Root and rhizosphere samples from the F1, F2, F3 and M1 sites were processed as in Schneider-  
118 Maunoury *et al.* (2018, 2020). Briefly, the ITS2 region of the ribosomal operon was amplified using the  
119 primers ITS86-F (3'-GTGAATCATCGAATCTTGAA-5') and ITS4 (see above) which favor the detection of  
120 Ascomycota and Basidiomycota (the two phyla containing ectomycorrhizal fungi) over Glomeromycota  
121 (Waud *et al.*, 2014; Op De Beeck *et al.*, 2014). PCR products were purified, pooled in equimolar pools  
122 and sequenced with an Ion Torrent sequencer (Life Technologies, Carlsbad, USA).

123 Samples from Gaillac sites were disrupted with a TissueLyser II using two inox beads (3x30s at 30 Hz).  
124 Total gDNA was then extracted using the Qiagen Plant Kit following the manufacturer instructions and  
125 stored at -20°C. We also performed extractions with no root samples as negative controls. All gDNA  
126 extracts were purified to remove potential PCR inhibitors. To do so, gDNA was mixed with Ampure XP  
127 (Beckman Coulter Inc., USA) solution in a 1 (gDNA) : 1.8 (Ampure) (v:v) ratio. The reaction plate was  
128 then placed on a magnetic plate to separate beads from the solution. The supernatant was removed  
129 and beads were washed with 70% EtOH two times. gDNA was then resuspended in EB buffer. Purified  
130 gDNA concentrations were measured with PicoGreen and all gDNAs were diluted to 3.5 ng/µL. The  
131 ITS2 region of the ribosomal operon was amplified using barcoded ITS286-F/ITS4 primers in triplicate  
132 with the DFS-Taq (Bioron Life Science, Germany). The PCR mixture consisted in 2.5 µL of Incomplete  
133 Buffer (10x), 0.5 µL of MgCl<sub>2</sub>, 2.5 µL of 3% BSA, 0.5 µL dNTPs (10 mM each), 0.75 µL of each primer (at  
134 10 µM), 2U of Bioron DFS-Taq, 3 µL of DNA (3.5 ng/µL) and 14.1 µL of H<sub>2</sub>O. The cycling conditions were  
135 as follow: 10 min at 95°C (initial denaturation), 35 steps of denaturation (95°C, 30s), annealing (56.5°C,  
136 30s), elongation (72°C, 30s) and a final elongation at 72°C for 10 min. We also added PCR negative  
137 controls for which DNA was replaced by water. PCRs products were then checked on a 2% agarose gel  
138 and purified using AMpure XP solution with a 1:1 (v:v) ratio as described before. Purified PCRs products  
139 concentration was measured with PicoGreen and pool in equimolar quantity. Equimolar pool was also  
140 purified. Sample pools were sequenced using a 2x250 Miseq technology on an Illumina platform by  
141 Fasteris SA (Switzerland).

142

#### 143 **Methods S2.2: Bioinformatic analysis of amplicon sequences**

144 As fungal communities of samples from sites across France (F1, F2, F3 and M1) and Gaillac sites (MF1,  
145 MF2, F4, F5, M2) were obtained using two different sequencing technologies, the first processing steps  
146 were slightly different. Samples from the first four sites were sequenced in distinct IonTorrent runs.  
147 Reads were then assembled and demultiplexed on the IonTorrent platform. Sequences were quality  
148 checked, with less stringent parameters in order to keep a large sequencing depth (--fastq\_maxns 1, -  
149 -fastq\_maxee 3, --fastq\_minlen 200). For samples from Gaillac sites, paired-end reads were assembled  
150 and quality checked (--fastq\_maxns 0, --fastq\_maxee 2) using cutadapt (Martin, 2011) and then  
151 demultiplexed (keeping only sequences longer than 200 pb).

152 Assembled and demultiplexed reads of the 9 sites were then processed altogether. Reads were  
153 dereplicated and clustered as classical 97% sequence similarity Operational Taxonomic Units (OTUs)  
154 using VSEARCH (Rognes *et al.*, 2016). Sequences were checked for the presence of chimeras (--  
155 uchime\_denovo). The taxonomy was assigned with VSEARCH against the Unite v8.3 database (Nilsson  
156 *et al.*, 2019). Reads were filtered in order to keep only non-chimeric sequences of > 200 pb, with a  
157 total abundance of at least 10 and a spread (i.e., the number of samples where the read is present)

158 superior or equal to 1. We used the *decontam* algorithm (Rivera *et al.*, 2011) to remove the potential  
159 contaminants in the Gaillac samples, using both algorithms (*prevalence* and *frequency*). First, we used  
160 the *prevalence* algorithm using the negative extraction and PCR controls with a stringent threshold of  
161 0.5. We then used the *frequency* algorithm using default parameters. A few more filters were applied  
162 to all datasets: we removed samples less than 2 000 fungal reads, OTUs with less than 5 reads per  
163 sample and OTUs representing less than 0.5% of the reads per sample.  
164 We inferred functional fungal traits using the FUNGuild database (Nguyen *et al.*, 2016). We only  
165 considered “Probable” and “Highly Probable” assignations and classified the others as “Unknown”.  
166 OTUs assigned to multiple trophic guilds (e.g., Saprotoph-Plant Pathogen) were grouped in the  
167 category “Others”.

168 **Supplementary Methods 3: Statistical analysis of fungal communities**  
169  
170 Amplicon sequencing data were processed using the R software (R Core Team, 2023) and the package  
171 *phyloseq* (McMurdie and Holmes, 2013).  
172  
173 **Methods S3.1: Influence of the sites and plant host on fungal communities**  
174 In order to test for differences in EcM relative abundance between sites, we used pairwise Wilcoxon  
175 rank test (*pairwise\_wilcoxon\_test*, *rstatix* package; Kassambara, 2023). We used  $\beta$ -diversity metrics to  
176 determine the influence of the location and the plant host family on total and EcM fungal communities.  
177 To do so, we computed Bray-Curtis distances from both relative abundances, as they may perform  
178 better for community comparisons (Gloor *et al.*, 2017; McKnight *et al.*, 2019), and Hellinger-  
179 transformed data to correct for variability in sampling depth (Legendre & Gallagher, 2001). We  
180 computed PERMANOVA with 10,000 permutations using the *adonis2* function of the *vegan* R package  
181 (Oksanen *et al.*, 2013). The formula used was: *distance matrix ~ site x family*. Analyses were run  
182 separately for the four sites across France and Gaillac sites as fungal communities were sequenced  
183 with different technologies.  
184  
185 **Methods S3.2: Differential abundances analyses of OTUs between environment types in Gaillac sites**  
186 In order to test whether some fungal OTUs were significantly more abundant in one of the three  
187 environments of the Gaillac sites (*i.e.*, forest, meadow and forest edge), we ran several differential  
188 abundances analysis as advised in Nearing *et al.* (2022): *LEfSE* (Segata *et al.*, 2011), *ANCOM-BC* (Lin &  
189 Peddada, 2020) and *ALDEx* (Fernandes *et al.*, 2013). OTUs were considered differentially abundant in  
190 one environment only if they were identified as differentially abundant with the three methods. We  
191 represented differentially abundant OTUs based on the Linear Discriminant Analysis score (LDA)  
192 computed in the *LEfSE* procedure.  
193  
194 **Methods S3.3: Constructing and characterizing bipartite networks of interactions between EcM fungi**  
195 **and non-EcM plants**  
196 We built bipartite networks in order to search for patterns of associations between EcM fungi and non-  
197 EcM-plants and to compare their structure to available knowledge on true mycorrhizal associations.  
198 We used the *bipartite* R package (Dormann *et al.*, 2008) to build plant/EcM fungi bipartite networks.  
199 We built the networks at both fungal genera/plant family and fungal OTUs/plant species levels to see  
200 if observed patterns were consistent across different taxonomic levels. We built one network for the  
201 four sites across France (regional scale) and one for Gaillac sites (local scale). Furthermore, we built  
202 one network for each site separately to ensure that observed patterns are not linked to differences

203 between sites, in particular modularity and specialization which can be linked to differences between  
204 habitats. We plotted the bipartite graphs using the *plotweb* function (*bipartite* package). To  
205 characterize the networks' structure, we computed several metrics: (i) nestedness (weighted NODF,  
206 *networklevel* function), (ii) modularity (Q, Beckett's algorithm from the *computeModules* function) and  
207 (iii) specialization ( $H_2'$ ; *H2fun* function). (i) In nested networks, specialists interact mainly with  
208 generalists and *vice versa* (Bascompte *et al.*, 2003). (ii) Modularity arises from subsets of preferential  
209 associations, which may be linked to reciprocal adaptations within modules (Dormann *et al.*, 2017).  
210 (iii) Finally,  $H_2'$  measures the level of specialization in interactions among plant and fungus and allows  
211 comparisons between networks of different size (Blüthgen *et al.*, 2006).  $H_2'$  varies between 0 (no  
212 network specialization) to 1 (network fully specialized). In order to test whether the properties of the  
213 bipartite networks were significantly different than expected by chance (that is, different from random  
214 patterns of associations), we generated, for each network, 1,000 random networks using the  
215 *quasiswap* null model algorithm (*permatswap* function), a stringent algorithm that keeps both  
216 connectance and marginal sums of the original network constant. Networks are considered nested (or  
217 anti-nested) if more than 97.5% of the generated networks have a lower (resp. higher) weighted NODF  
218 than the real network ( $p<0.025$ ). Similarly, networks are considered significantly modular and  
219 specialized if more than 97.5% of the generated networks have lower Q and  $H_2'$  values, respectively  
220 ( $p<0.025$ ).

221

222 **Methods S3.4: Comparisons of rhizosphere and root EcM fungal communities**

223 In order to quantify and characterize a potential root filter applied to rhizospheric EcM fungi, we  
224 compared the EcM  $\alpha$ -diversity between compartments for each species by computing the Shannon  
225 index and tested for significant differences between compartments using Tukey's Honest Significant  
226 Differences after running the following linear regression: *Shannon index* ~ *plant species* x  
227 *compartment*. Normality and homoscedasticity of the Shannon index were checked using diagnostic  
228 plots. We also compared the composition of the total and EcM fungal communities in the two  
229 compartments using PERMANOVA (*adonis2* function of the *vegan* R package, 10,000 permutations)  
230 with the following model: *distance matrix* ~ *compartment* x *plant species*. As detailed before, distance  
231 matrices were computed using the Bray-Curtis distance based on both relative abundances and  
232 Hellinger-transformed data. Differences in composition were represented using Non-Metric  
233 Multidimensional Scaling (NMDS). Pairs of samples are connected by a grey line. For each species, we  
234 identified the number of OTUs shared (or not) between the two compartments and computed their  
235 relative read abundance in the EcM community (threshold of one read). Finally, we assessed if some  
236 EcM fungal genera are significantly more abundant (or not) in one of the two compartments using

237 differentially abundant analysis. To do so, we used the Linear Discriminant Analysis Effect Size  
238 procedure (*LEFsE*; Segata *et al.*, 2011).

239 **Supplementary Methods 4: Fluorescence *in situ* hybridization (FISH) and microscopy**  
240 **detection of *Russula* hyphae**

241  
242 **Methods S4.1: Design of rRNA probes specific to *Russula* spp. for FISH and microscopy observations**  
243 Oligonucleotide probes were designed to target the 18S rRNA of *Russula* genus including the *Russula*  
244 fruitbodies harvested in areas producing *Russula* caprophores in the Gaillac sites. *Russula* 18S  
245 ribosomal DNA (rDNA) sequences were obtained from fruitbodies harvested on and outside productive  
246 areas and from genomic data published in NCBI GenBank or Mycocosm databases (The Fungal  
247 Genomics Resource-JGI) (cf. Supp. File 1 to see accessions used). *Russula* 18S rRNA sequences were  
248 aligned using the free Multalin algorithm (Corpet, 1988) along with 18S rRNA sequences of a selection  
249 of several orders in Agaromycetes and Russulaceae family. The alignment was scanned visually to  
250 detect regions of sequence homology suitable for *Russula* genus-specific probes, i.e., conserved within  
251 the *Russula* genus but with differences (mismatches) compared to other genera. We identified 6  
252 regions exhibiting polymorphisms which could therefore be used as a basis for designing probes  
253 targeting *Russula* spp. (or including closely related genera in the Russulaceae family). Physical  
254 accessibility of probes to these regions was assessed using reference maps of probe accessibility and  
255 sensitivity available in *Prymenisum parvum* (Metfies and Medlin, 2008). The specificity of potential  
256 probes was tested *in silico* using iterative BLAST searches with low stringency algorithm parameters in  
257 the GenBank and SILVA databases. Taking into account the number of mismatches of the designed  
258 probes and the *in silico* accessibility and specificity, we selected 2 probes: RUS899 and RUS101 (see  
259 table below for sequences). FISH-probes were commercially synthesized by Biomers (Biomers.net,  
260 Ulm/Donau, Germany) including 5'-end labeled with ATTO fluorochromes and stored in sterile DNA-  
261 grade water at -20°C.

Name	Sequence	Fluorescent dye
EUK516	ACCAGACTTGCCCTCC	ATTO565
NON-EUK516	GGAGGGCAAGTCTGGT	ATTO565
RUS101	ATGTAGAAAGGTATCATCAAAT	ATTO633
RUS899	CGCAATAGTTGTCTGCGTAAAT	ATTO633
NON-RUS899	ATTACGCAAGACAAACTATTGCG	ATTO633

262  
263  
264 **Methods S4.2: In vitro specificity test of the newly designed probes**  
265 Strains of *Phanerochaete chrysosporium* RP78, *Lactarius quietus* S05C, *Russula luteotacta* 201811 RL,  
266 *Russula* sp. AT 0111 were cultivated on P5 medium (Paschelwski agar medium 5, Di Battista *et al.*,  
267 1996) in order to test probes' sensitivity and specificity *in vitro* and to set up confocal acquisition

parameters. All strains were supplied by the UMR IAM 1136 isolates collection grown for several days in P5 medium at 25°C. When fungal elements became visible by eye, the hyphae were harvested, washed with PBS 1x, fixed in the 3% PFA fungi fixation solution for 24 h (see Supp. File 2 for details on all reagents used), washed in PBS and finally stored at -20°C in 50% ethanol-PBS 1x until use. Moreover, different part of fruitbodies harvested *in situ* (cape and/or stipe) of *Russula* spp. and two other undetermined fungi species (C1 and C2) harvested on and outside forest edges were included in the specificity test. *Russula* sp. (stipe and cape), and undetermined fungi C1 and C2 were razor blade cut, rinsed in PBS 1x and fixed in the fungi fixation solution as for pure culture fungi. For FISH, fruitbodies and mycelium samples were gradually dehydrated in an ethanol series prepared in sterile ultrapure water (50%, 70%, 96% and 100%) 5 min each and rehydrated in an ethanol series (70%, 50%, 30%, 10%) prepared in PBS-T 5 min each before a last PBS-T bath. Samples were treated for 15 min at 30°C with FCWE digestion solution to weaken fungal cell walls before prehybridization at 46°C during 10 min. The prehybridization buffer was then replaced with a hybridization buffer containing the probe(s) (0.35pmol/μL of hybridization solution each) during 2h at 46°C. After a stringent wash in the washing solution during 10 min at 46°C followed by PBS 1x bath, sample were mounted in antifade solution, and visualized on a laser scanning confocal microscope (Zeiss LSM980; Carl Zeiss, Oberkochen, Germany) equipped with an Airyscan2 detector and coupled to ZEN Blue 3.3 software (Carl Zeiss). In some cases, the cultivated hyphae have been placed and fixed on Poly-L-lysine coated slides (Sigma-Aldrich, St. Louis, MO, USA) before applying the FISH protocol. Fungal samples were co-hybridized with either the universal eukaryote probe EUK516 and with one of the following probes: sense *Russula* probes (RUS899/RUS101), non-sense *Russula* probe (NonRUS899) or none sense EUK516 probe, using a combination of distinct fluorescent dyes.

290

291 **Methods S4.3: Hybridization and observation of *Russula* spp. hyphae in roots of non-EcM plant  
292 species**

293 To visualize *Russula* fungi within non-EcM plant roots, we set up a FISH experiment. Roots samples  
294 harvested in September 2021 and July 2023 (Table S1) were washed carefully several times in water  
295 and PBS 1x in order to eliminate the rhizospheric soil. Root pieces collected were cut into two  
296 consecutive segments of 1-cm long. One was immediately immersed in the plant fixation solution (PFA  
297 4%) and incubated overnight at 4°C to fix RNAs. Samples were then rinsed three times in PBS 1x and  
298 progressively dehydrated in a series of ethanol solutions (10%, 30% and 50%) during 15 min each. The  
299 root segments were stored in the sample storage solution and kept at -20°C for further analyses.  
300 Segments for which *Russula* sequences were detected (Methods S2) were used for FISH experiments.  
301 We used two types of probes, both targeting 18S rRNA. One is the universal eukaryote probe EUK516,  
302 which targets the 18s rRNA of eukaryotic cells (Amann *et al.*, 1990; see above for probes sequences)

303 coupled with ATTO-565 dye (Biomers, Germany), hereafter called “EUK565”. The other probe was  
304 either one of the two newly designed probes targeting specifically *Russula* 18S rRNA (RUS889 and  
305 RUS101, Methods S4.1) coupled with ATTO-633 dye (Biomers, Germany). As in Schneider-Maunoury  
306 *et al.* (2020), fluorochromes were chosen to minimize the autofluorescence of the fungi and plant root  
307 tissues. In order to visualize plant and fungal cell walls, the dye SR2000 (Renaissance Chemicals) was  
308 added to the hybridization buffer.

309 Selected samples were treated for 1h at 30°C with PCWE digestion cocktail 1x mixed with FCWE  
310 digestion solution 1x to weaken plant and fungal cell walls. After rinsing them into PBS-T, samples were  
311 then treated with 0.08µg/µl of Proteinase K during 30min at 37°C. The proteinase K reaction was  
312 stopped by replacing the solution by Glycine working buffer during 2 min and the samples were  
313 incubated 30 min in the post fixative solution, rinsed and prehybridized at 46°C during 30 min. The  
314 prehybridization buffer was replaced with hybridization buffer containing the probe(s) (0.35pmol/µL  
315 of hybridization solution each) during 2h at 46°C. After a stringent wash in the washing solution during  
316 10 min at 46°C, sample were mounted in antifade solution mixed with 0.1% of SR2000 (Renaissance  
317 Chemicals).

318 The *FISH*-stained root samples were further mounted with Slowfade Diamond Antifadent (Molecular  
319 Probes, Eugene, OR, USA, ThermoFisher, cat. no. S36963) and stored at 4°C over night until observation  
320 with a laser scanning confocal microscope (LSM 980 Zeiss microscope) equipped with an EC-Plan  
321 Neofluar 10x/0.3 dry objective, a W Plan-Apochromat 20x/1.0 water and a Plan-Apochromat 63x/1.4  
322 oil objective. The Airyscan 2 module was used for acquisitions using the multiplex 4Y mode. Probes  
323 labelled with ATTO565 or ATTO633 dyes were excited at 568nm or 647 nm wavelengths respectively  
324 and detected with a bandpass filter (570-630 nm and 660-720 nm). The cell wall fluorescent dye  
325 SR2000 was visualized with a laser excitation at 405 nm wavelength and recorded with a bandpass  
326 filter (420-477nm). For each field of view, an appropriate number of optical sections were acquired  
327 with a Z-step of 0.15 to 1 µm. Airyscan images were reconstructed and analysed using ZEN Blue 3.5,  
328 ZEN 2.1 LITE black software (Zeiss), the Vision4D 3.0.1 software (arivis AG, Germany) or the free  
329 software FIJI-ImageJ. Hybridization signals obtained on non-ECM roots samples were successfully and  
330 specifically detected for EUK516 and the sense *Russula* probes and the same parameters (laser power  
331 and gain of detector) were used to image the control samples: samples without any probe or samples  
332 hybridized with the non-sense probes.

333 **Supplementary discussions (1-2)**

334

335 **Supplementary discussion 1: The structure of mutualist interactions' bipartite networks**

336 In order to further characterize the interactions between EcM fungi and non-EcM plants, we  
337 constructed the network of interactions between EcM fungi and non-EcM plants in Gaillac sites (local  
338 scale; Fig. 1d), in sites across France (regional scale; Fig. S5), and in each site individually. We assessed  
339 the topological properties of the networks by computing the commonly used modularity and  
340 nestedness (here weighted nestedness; Bascompte *et al.*, 2003; Olesen *et al.*, 2007). Modularity (that  
341 is, groups of species that interact preferentially) may arise in intimate interactions such as symbiotic  
342 mutualism or parasitism, resulting in reciprocal specialization (Olesen *et al.*, 2007) but may also be  
343 linked to environmental or geographic factors. Nestedness was thought to be a characteristic of  
344 mutualistic networks (Bascompte *et al.*, 2003) providing stability in the community. In a nested  
345 network, generalists tend to associate with specialists and *vice versa*. However, recent results show  
346 that nestedness is not reliable to predict if a network is mutualist (Pichon *et al.*, 2023 and citations  
347 hereafter).

348 Here, we show that the colonization of EcM fungi in roots of non-EcM plants results in a modular  
349 network in both Gaillac sites (Fig. 1d; Table S3) and sites across France (Fig. S5; Table S3). At the site  
350 level, modularity was frequently observed especially in networks at the fungal OTUs/plant species level  
351 (Table S3). Patterns of nestedness, non- and anti-nestedness were observed across sites with no clear  
352 tendency. The network of Gaillac sites was significantly nested (Table S3) while the network of sites  
353 across France was significantly anti-nested. Different mycorrhizal types tend to have contrasted  
354 network structures. For instance, arbuscular mycorrhizal fungi and plants tend to form nested  
355 networks (Chagnon *et al.*, 2012; Montesinos-Navarro *et al.*, 2012) with intermediate modularity (Toju  
356 *et al.*, 2014; Pölme *et al.*, 2018). EcM interactions on the contrary are often reported to form non- or  
357 anti-nested networks (Bahram *et al.*, 2014; Toju *et al.*, 2014; Roy-Bolduc *et al.*, 2016) though  
358 nestedness was observed in some cases (Peay *et al.*, 2007). Modularity was sometimes observed in  
359 EcM/plant networks but is not systematic (see previous studies). Anti-nestedness and modularity were  
360 also observed in epiphytic orchids mycorrhizal interaction networks (Martos *et al.*, 2012; Petrolli *et al.*,  
361 2022) and in ericaceous plant fungus networks (Toju *et al.*, 2016). Thus, mutualistic mycorrhizal  
362 associations result in diverse networks topologies depending on the mycorrhizal type(van der Heijden  
363 *et al.*, 2015). In this work, we find that EcM fungi colonizing non-EcM plants result in modular bipartite  
364 networks, with contrasted patterns of nestedness, fitting observations in true EcM fungi.

365 Furthermore, we assessed the specialization of EcM fungi and non-EcM plants networks using the H<sub>2</sub>',  
366 allowing comparisons between networks of different sizes (Blüthgen *et al.*, 2006). We found high  
367 degrees of specialization in both Gaillac sites and sites across France (Table S3). As with modularity,

specialization was often observed at the individual site level, in particular at the fungal OTUs/plant species level. Observed specialization was greater than in some mycorrhizal associations (Toju *et al.*, 2014; Perez-Lamarque *et al.*, 2022) but similar to that observed in grasses root endophytes (Kivlin *et al.*, 2022).

In this study, bipartite networks of interactions between non-EcM plant roots by EcM fungi are both modular and specialized, two correlated network properties (Dormann & Strauss, 2014). These properties were also observed within sites suggesting that they are not only linked to differences between sites but rather to preferential interactions between plants and fungi (Dormann *et al.*, 2017). These patterns may arise from several process such as one-sided adaptation or co-evolution (Dormann *et al.*, 2017).

378

### **379      Supplementary discussion 2: A rhizospheric host filtering of EcM fungi by non-EcM plants?**

380      We assessed the EcM community of roots of non-EcM plants from several families in different sites.  
381      Comparisons of EcM communities show significant differences between plant families (Fig. 1c; Fig. S3;  
382      Supp Table 2c,d). Furthermore, bipartite networks of interactions between non-EcM plants and EcM  
383      fungi are highly specialized and modular (Fig. 1d; Fig. S5; Table S3), even at the site level (Table S3),  
384      suggesting preferential interactions between groups of EcM fungi and non-EcM plants. Altogether,  
385      these results suggest a host filtering of EcM fungi. However, the comparison of rhizosphere and roots  
386      EcM communities in paired samples revealed no significant differences in EcM community composition  
387      between the two compartments (Fig. 2; Fig. S6; Table S5), though EcM fungi were much less abundant  
388      in roots than in rhizosphere (Fig. 2a).

389      This apparent discrepancy suggests that host filtering of EcM communities by non-EcM plants may  
390      occur both in rhizosphere and in roots. First, root exudates may shape EcM community composition in  
391      the rhizosphere. Knowledge acquired in true EcM associations demonstrate that plant exudates such  
392      as flavonoids or abietic acid may participate to EcM development and spores' germination in the  
393      rhizosphere (as reviewed in Garcia *et al.*, 2015; Martin *et al.*, 2016). In this study, we investigated roots  
394      (and rhizosphere) of plants forming arbuscular mycorrhizae (AM) or no mycorrhizae (NM) for which  
395      molecular dialogue with EcM fungi has not been investigated. As EcM plants, AM plants produce root  
396      exudates such as strigolactones that participate to AM fungal partners' recruitment (Bonfante &  
397      Genre, 2010), and thus shape the rhizosphere microbiome (Uroz *et al.*, 2019). It has been hypothesized  
398      that strigolactones may also be involved in EcM molecular dialogue (Garcia *et al.*, 2015) despite  
399      conclusive evidence. The rhizosphere is a complex and dynamic compartment within which root and  
400      fungal exudates are likely to influence the development of fungi (e.g., EcM fungi) and thus influence  
401      root mycobiota assembly, leading to differences between plant species.

402 Second, the ability of EcM fungi to colonize non-EcM roots may be limited, leading to a low abundance  
403 of EcM fungi in non-EcM roots compared to the rhizosphere (Fig. 2a). The fungal colonization in true  
404 mycorrhizal associations usually requires an important root remodeling to ensure access of root tissues  
405 to the fungal partner and reduced plant defenses. Reduction of plant defense during colonization is  
406 modulated by fungal exudates (*e.g.*, Small Secreted Proteins in EcM associations; Plett *et al.*, 2014;  
407 Martin *et al.*, 2016) ensuring a specific recognition of mycorrhizal fungi. The endophytic niche may  
408 facilitate and predispose plant and fungal adaptations allowing more specialized and complex  
409 interactions such as mycorrhizae, as stipulated by the ‘waiting-room’ hypothesis (Selosse *et al.*, 2009,  
410 2021).

411

412    **Supplementary Tables (1-7)**

413  
414    **Supplementary Table 1: Details on samples collected.**

415    Location, number of root samples, number of individuals, number of plant species/family and their  
416    corresponding analysis.

Location	Name	Date	Nb. root samples	Nb. individuals	Nb. species	Nb. family	Rhizospheric soil	Analysis
Orry-la-Ville (ORY)	Forest 1 (F1)	April 2019	18	18	4	3	18	Ion Torrent sequencing (ITS2)
Orsay (ORS)	Forest 2 (F2)	March 2019	16	16	4	4	16	Ion Torrent sequencing (ITS2)
Corrèze (TMEL)	Forest 3 (F3)	May 2016	59	59	7	7	-	Ion Torrent sequencing (ITS2)
Jardin des Plantes (JE)	Meadow 1 (M1)	June 2017	48 + 42	46	11	10	-	Ion Torrent sequencing (ITS2)
Gaillac	Edge 1 (MF1)	June 2021	141	141	30	13	-	Illumina sequencing (ITS2)
		September 2021	59	21	7	6	-	Illumina sequencing (ITS2) + FISH-microscopy
		July 2023	4 root systems	4	2	2	-	FISH-microscopy
	Edge 2 (MF2)	June 2021	38	38	10	7	-	Illumina sequencing (ITS2)
		September 2021	50	17	7	6	-	Illumina sequencing (ITS2) + FISH-microscopy
	Forest 4 (F4)	June 2021	16	16	4	4	-	Illumina sequencing (ITS2)
	Forest 5 (F5)		13	13	7	4	-	
	Meadow 2 (M2)		41	41	10	6	-	
<b>Total</b>			<b>557</b>	<b>433</b>	<b>42</b>	<b>17</b>	<b>34</b>	

417

418

419 **Supplementary Table 2: Plant host family and site of sampling influence both the total root  
420 mycobiota composition and the EcM mycobiota composition of non-EcM plants.**

421 Outputs of the PERMANOVA analysis (*adonis2* function *vegan* R package), performed using the Bray-  
422 Curtis distances computed from both relative abundance and Hellinger transformed data of the total  
423 fungal community (**a, b**) or the EcM community (**c,d**) only with 10 000 permutations. The analyses were  
424 performed on the samples collected in (**a**), (**c**) the areas producing *Russula* spp. fruitbodies and the  
425 adjacent forest and meadow and in (**b**), (**d**) four natural environments across France. *family*  
426 corresponds to the plant host family. *environment* corresponds to the area where samples from (a),  
427 (c) were collected (areas producing *Russula* fruitbodies, forest or meadow). *location* corresponds the  
428 four natural environments of (b), (d) (cf. Table S1).

Total fungal community							
(a)	Variable	R <sup>2</sup>	p-value	(b)	Variable	R <sup>2</sup>	p-value
Relative abundance	family	0.15	10 <sup>-3</sup> (***)	Relative abundance Hellinger transformation	family	0.32	10 <sup>-4</sup> (***)
	site	0.06	10 <sup>-3</sup> (***)		site	0.05	10 <sup>-4</sup> (***)
	interaction	0.06	10 <sup>-4</sup> (***)		interaction	0.01	6x10 <sup>-4</sup> (***)
	Residuals	0.73	-		Residuals	0.63	-
	family	0.17	10 <sup>-4</sup> (***)		family	0.37	10 <sup>-4</sup> (***)
	site	0.08	10 <sup>-4</sup> (***)		site	0.06	10 <sup>-4</sup> (***)
	interaction	0.06	10 <sup>-4</sup> (***)		interaction	0.01	1.9x10 <sup>-3</sup> (***)
	Residuals	0.69	-		Residuals	0.57	-
EcM fungal community							
(c)		R <sup>2</sup>	p-value	(d)		R <sup>2</sup>	p-value
Relative abundance	family	0.12	10 <sup>-4</sup> (***)	Relative abundance Hellinger transformation	family	0.34	10 <sup>-4</sup> (***)
	site	0.03	10 <sup>-4</sup> (***)		site	0.08	10 <sup>-4</sup> (***)
	interaction	0.04	10 <sup>-4</sup> (***)		interaction	0.01	0.09
	Residuals	0.82	-		Residuals	0.57	-
	family	0.13	10 <sup>-4</sup> (***)		family	0.36	10 <sup>-4</sup> (***)
	site	0.04	10 <sup>-4</sup> (***)		site	0.09	10 <sup>-4</sup> (***)
	interaction	0.04	10 <sup>-4</sup> (***)		interaction	0.01	0.05
	Residuals	0.78	-		Residuals	0.57	-

430 **Supplementary Table 3: Bipartite networks metrics and significance.**

431 We constructed bipartite networks of interactions between EcM fungi and non-EcM plants at two  
 432 taxonomic levels: fungal genera and plant families **(a)** fungal OTUs and plant species **(b)**. At each  
 433 taxonomic level, we constructed one network for the Gaillac sites (local scale), one network for the  
 434 sites across France (regional scale), and one network per site. We characterized their structure using  
 435 several network metrics (specialization, modularity and weighted nestedness) computed with the  
 436 *bipartite* R package. We then tested whether obtained values are significantly different than expected  
 437 by chance using null models ([Methods S3.3](#)).

438

(a)	Genera/Families			
	H <sub>2</sub> '	Q	wNODF	C
<b>France</b>	<b>0.80*</b>	<b>0.56*</b>	<b>14.6* (-)</b>	0.27
M1	0.89	0.35	1.35	0.67
F1	<b>0.87*</b>	<b>0.59*</b>	36.7	0.63
F2	0.59	0.41	45.5	0.52
F3	0.88	0.48	<b>32.2* (+)</b>	0.39
<b>Gaillac</b>	<b>0.44*</b>	<b>0.33*</b>	<b>47.5* (+)</b>	0.43
M2	<b>0.53*</b>	<b>0.45*</b>	51.6	0.60
F4	<b>0.50*</b>	<b>0.41*</b>	44.5	0.68
F5	<b>0.85*</b>	<b>0.45*</b>	<b>30.9* (-)</b>	0.63
MF1	<b>0.43*</b>	<b>0.27*</b>	<b>51.3* (+)</b>	0.49
MF2	0.38	0.26	40.6	0.47

(b)	OTUs/Species			
	H <sub>2</sub> '	Q	wNODF	C
<b>France</b>	<b>0.85*</b>	<b>0.73*</b>	2.94	0.10
M1	<b>0.82*</b>	<b>0.58*</b>	19.9	0.37
F1	0.65	0.43	5.12	0.48
F2	<b>0.77*</b>	<b>0.51*</b>	5.64	0.47
F3	<b>0.82*</b>	0.52	5.71	0.32
<b>Gaillac</b>	<b>0.64*</b>	<b>0.55*</b>	<b>22.1* (+)</b>	0.20
M2	<b>0.73*</b>	<b>0.59*</b>	8.32	0.28
F4	<b>0.77*</b>	<b>0.52*</b>	9.83	0.52
F5	<b>0.89*</b>	<b>0.72*</b>	4.75	0.30
MF1	<b>0.71*</b>	<b>0.62*</b>	<b>19.7* (+)</b>	0.25
MF2	<b>0.69*</b>	<b>0.58*</b>	<b>22.7* (+)</b>	0.40

439

440 **Supplementary Table 4: Percentage of OTUs shared (or not) between rhizosphere and roots per**  
 441 **species and their contribution to the EcM community.**

442 For each species, we determined the percentage of OTUs found only in rhizosphere samples, shared  
 443 between rhizosphere and roots and found only in roots (number on the left). We also computed the  
 444 proportion of the EcM community that these represent (number on the right). For instance, 26% of  
 445 EcM OTUs are shared between rhizosphere and roots samples of *A. maculatum*, but these represent  
 446 66% of the total EcM reads.

447

	Rhizosphere (%)	Shared (%)	Roots (%)	Total number of EcM OTUs
<i>Arum maculatum</i>	73 / 34	26 / 66	1.3 / <1	74
<i>Convallaria majalis</i>	29 / 20	60 / 80	10 / <1	48
<i>Euphorbia</i> sp.	49 / 7	49 / 93	2.3 / <1	43
<i>Ficaria verna</i>	30 / 31	62 / 69	8 / <1	37
<i>Galium aparine</i>	51 / 8	38 / 81	11 / 11	37
<i>Mercurialis perennis</i>	47 / 15	50 / 85	2.8 / <1	36
<i>Poa</i> sp.	25 / <1	65 / 99	10 / <1	40

448 **Supplementary Table 5: Rhizosphere and roots have similar EcM mycobiota composition.**

449 Outputs of the PERMANOVA analysis (*adonis2* function *vegan* R package) performed using both  
 450 relative abundance and Hellinger transformed data with 10 000 permutations. The analyses were  
 451 performed on the samples collected in the ORS and ORY sites. (a) Analysis of the total fungal  
 452 community. (b) Analysis of the EcM fungal community. *species* corresponds to the plant host species  
 453 and *compartment* to the plant compartment (rhizosphere or root). *interaction* is the interaction term  
 454 between the two variables (*species* x *compartment*).

(a)	Variable	R <sup>2</sup>	p-value	(b)	Variable	R <sup>2</sup>	p-value
<b>Relative abundance</b>	species	0.16	10 <sup>-4</sup> (***)	<b>Relative abundance</b>	species	0.27	10 <sup>-4</sup> (***)
	compartment	0.06	10 <sup>-4</sup> (***)		compartment	0.02	0.12
	interaction	0.12	10 <sup>-4</sup> (***)		interaction	0.06	0.88
	Residuals	0.66	-		Residuals	0.65	-
<b>Hellinger transformation</b>	species	0.22	10 <sup>-4</sup> (***)	<b>Hellinger transformation</b>	species	0.23	10 <sup>-4</sup> (***)
	compartment	0.10	10 <sup>-4</sup> (***)		compartment	0.01	0.75
	interaction	0.10	10 <sup>-4</sup> (***)		interaction	0.06	0.98
	Residuals	0.57	-		Residuals	0.70	-

455

456 **Supplementary Table 6: Results of the sensitivity and specificity test of the newly designed probes**  
 457 **RUS899 and RUS101.**

458 In order to test for the sensitivity and specificity of the newly designed probes RUS101 and RUS899,  
 459 we hybridized fungi collected from pure cultures or from samples collected *in situ*. + and – signs  
 460 characterize the intensity of the fluorescence signal.

Tested probes	<i>Phanerochaete</i> sp.	<i>Lactarius quietus</i>	<i>Russula luteotacta</i>	<i>Russula</i> sp. <i>in vitro</i>	<i>Russula</i> sp. <i>in situ</i>	<i>Fungi</i> sp. 2 C2	<i>Fungi</i> sp. 1 C1
	Pure cultivated hyphae	Pure cultivated hyphae	Pure cultivated hyphae	Pure cultivated hyphae	Harvested ascocarp (cape)	Harvested Ascocarp	Harvested Ascocarp
EUK516	++	++	++	++	++	++	++
RUS101	-	+/-	+	-	+	NA	NA
RUS899	-	+(+)	+	+(+)	++	-	-
NONRUS506	NA	NA	NA	NA	-	-	-/+

461  
 462  
 463 **Supplementary Table 7: Details on plant host investigated for FISH detection collected.**  
 464 Information regarding potential plant host investigated for the presence of *Russula* spp. hyphae. Plant  
 465 species, sampling date, probes used for hybridization are given and whether *Russula* spp. hyphae could  
 466 be identified within the roots.

Plant species	Sampling date	Probes	Detection of <i>Russula</i> spp. hyphae (Y/N)
<i>Ranunculus bulbosus</i>	Sept. 2021	Rus899-ATTO633/Euk51-ATTO565 & Rus101-ATTO633/Euk51-ATTO565	Y
<i>Carex</i> sp.	Sept. 2021	Rus899-ATTO633/Euk51-ATTO565	N
<i>E. amygdaloides</i>	Sept. 2021	Rus899-ATTO633/Euk51-ATTO565	N
<i>P. officinaria</i>	Sept. 2021	Rus899-ATTO633/Euk51-ATTO565	N
	July 2023	Rus101-ATTO633/Euk51-ATTO565	Y/N
<i>Carduus pycnocephalus</i>	July 2023	Rus101-ATTO633/Euk51-ATTO565	Y

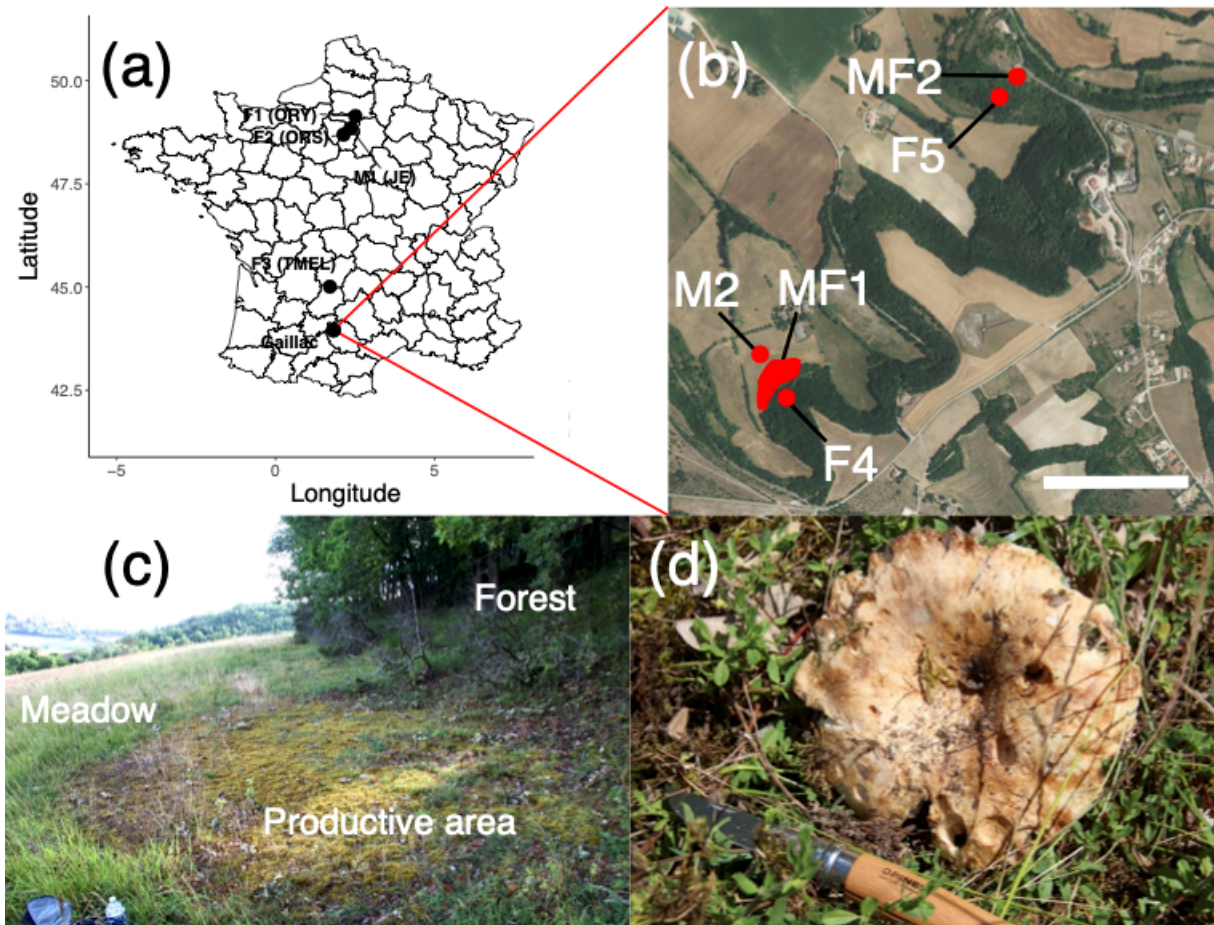
467

468 **Supplementary Figures (1-11)**

469

470 **Supplementary Figure 1: Location of the sampling sites and details of the Gaillac sites.**

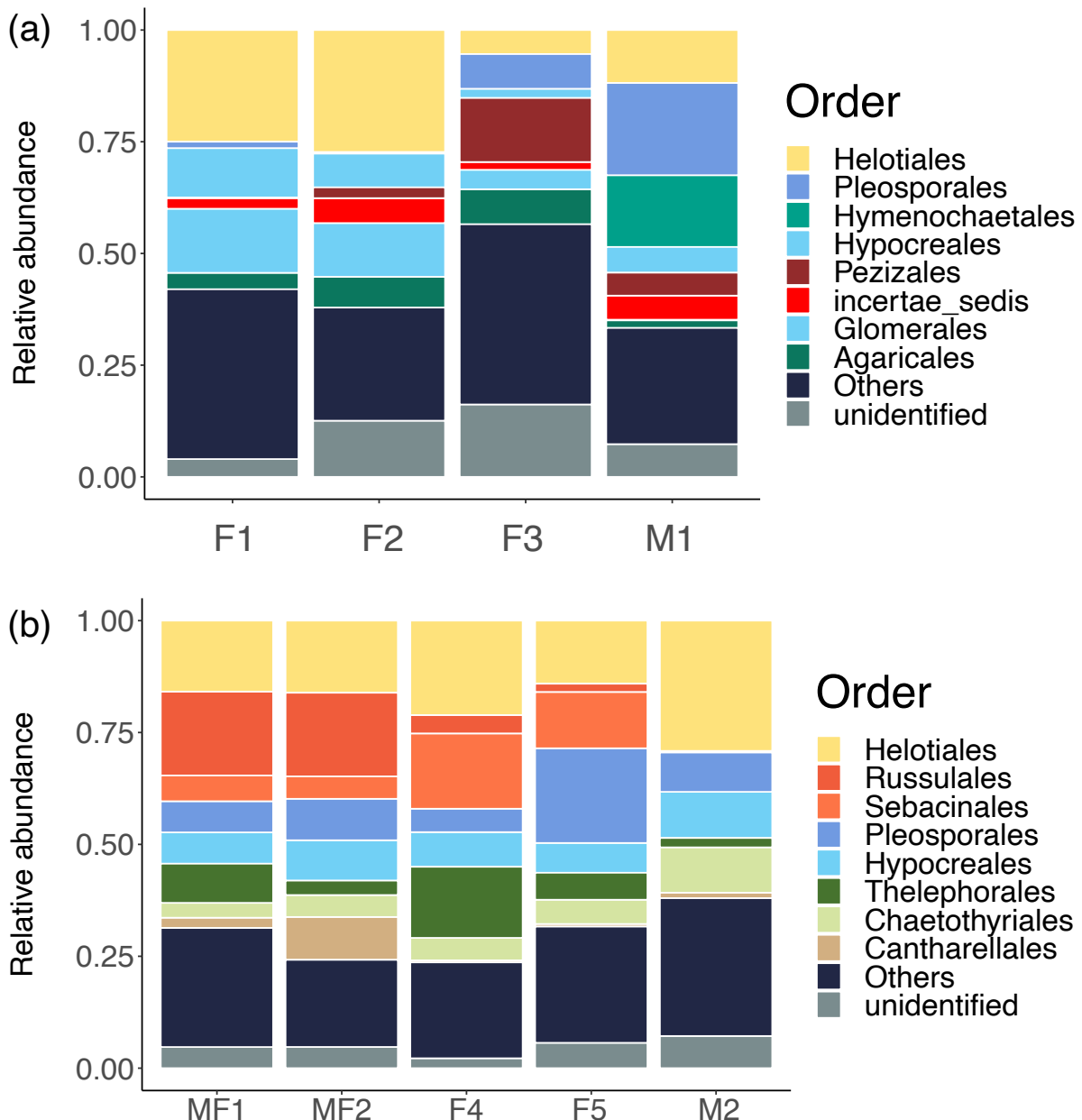
471 We sampled roots of non-EcM plant species in areas in several sites across France in forests (F) and  
472 meadows (M). In Gaillac, we also collected plants in edges of forests where abundant fruitbodies of  
473 *Russula* spp. were observed (MF). **(a)** Location of the sites in France. **(b)** Details on the location of the  
474 five Gaillac sites. Scale bar: 400 m. © IGN **(c)** Area producing *Russula* spp. fruitbodies (MF) and the  
475 adjacent forest (F) and meadow (M). **(d)** *Russula* sp. fruitbodies observed in June 2021 when sampling  
476 non-EcM roots. F: Forest; M: Meadow; MF: forest edge.



477

478

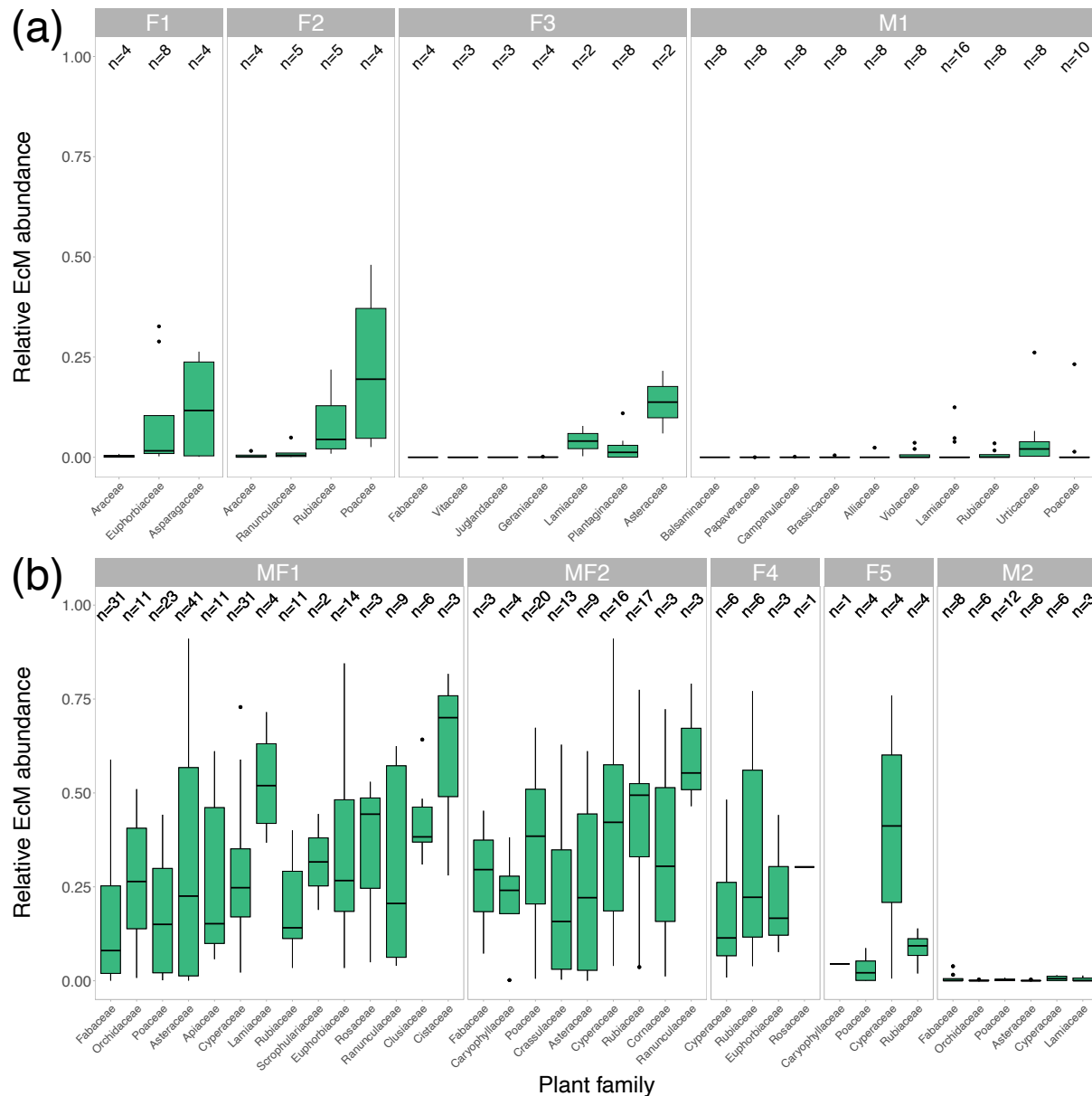
479 **Supplementary Figure 2: Total root mycobiota of non-EcM plants harvested in several sites in France.**  
 480 We described the root mycobiota of several non-EcM plants species in 9 sites across France using ITS2  
 481 amplicon sequencing. **(a)** Root mycobiota of plants collected in four sites across France. F: forest; M:  
 482 meadow. **(b)** Root mycobiota of plants collected in five sites near Gaillac, France. MF: sites at the edge  
 483 of the forest; F: forest; M: meadow.



484  
 485

486 **Supplementary Figure 3: The proportion of EcM fungi in roots of non-EcM plant roots varies**  
 487 **according to the plant host family and site.**

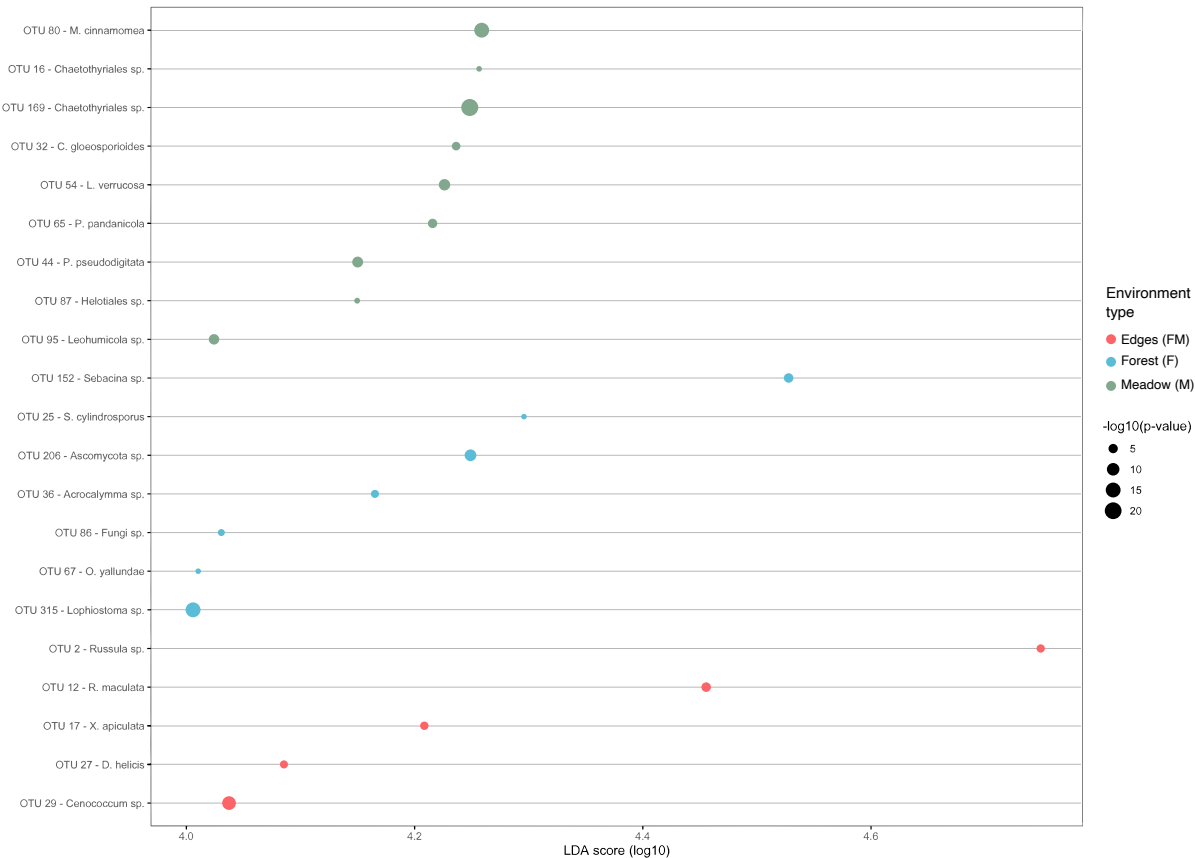
488 Boxplot of the proportion of EcM fungi by host family and by location. **(a)** Non-EcM plants collected in  
 489 the four sites across France. **(b)** Plants collected in the five Gaillac sites.



490  
 491

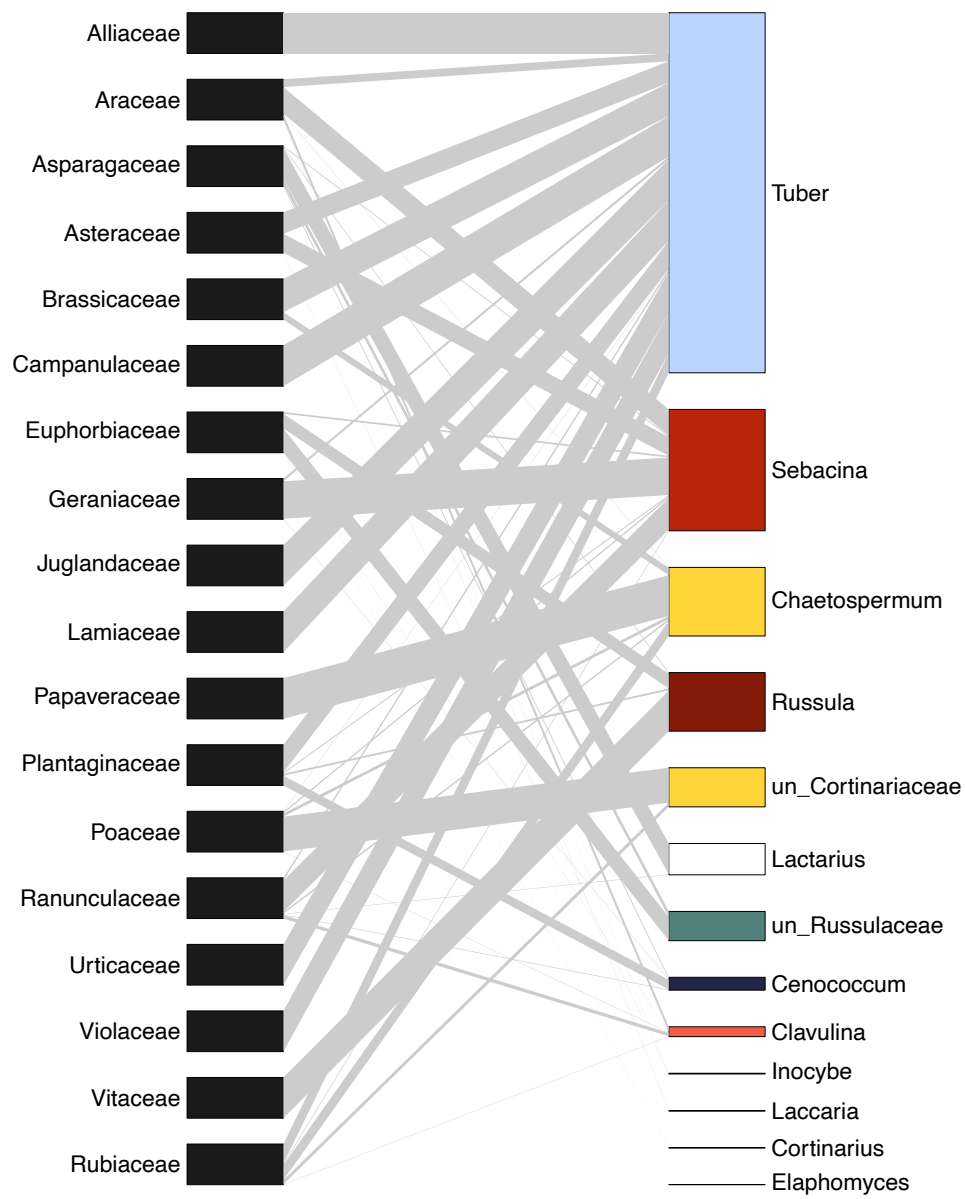
492 **Supplementary Figure 4: Forests, meadow and forest edges from Gaillac sites are characterized by**  
 493 **OTUs differentially abundant.**

494 Differentially abundant OTUs between the three environment types of Gaillac sites: forest, meadow  
 495 and forest edges. The x-axis corresponds to the Linear Discriminant Analysis score (LDA score)  
 496 computed with the *LEfSE* method, and the size of the dots is proportional to the *p-value*:  $-\log(p\text{-value})$ .



497

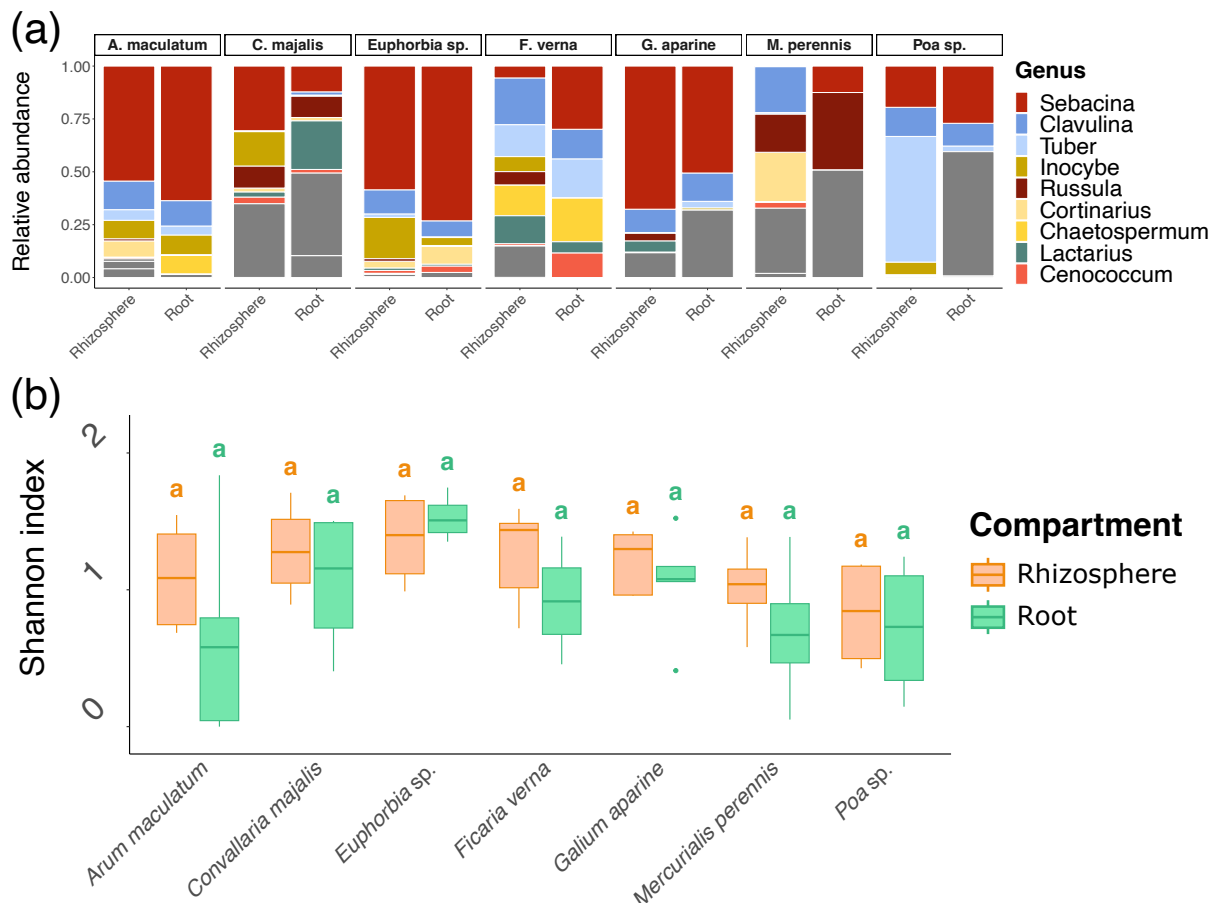
498 **Supplementary Figure 5: Bipartite network of interactions between plant families and fungal EcM**  
499 **genera across the four sites in France (F1, F2, F3 and M1).**



500  
501

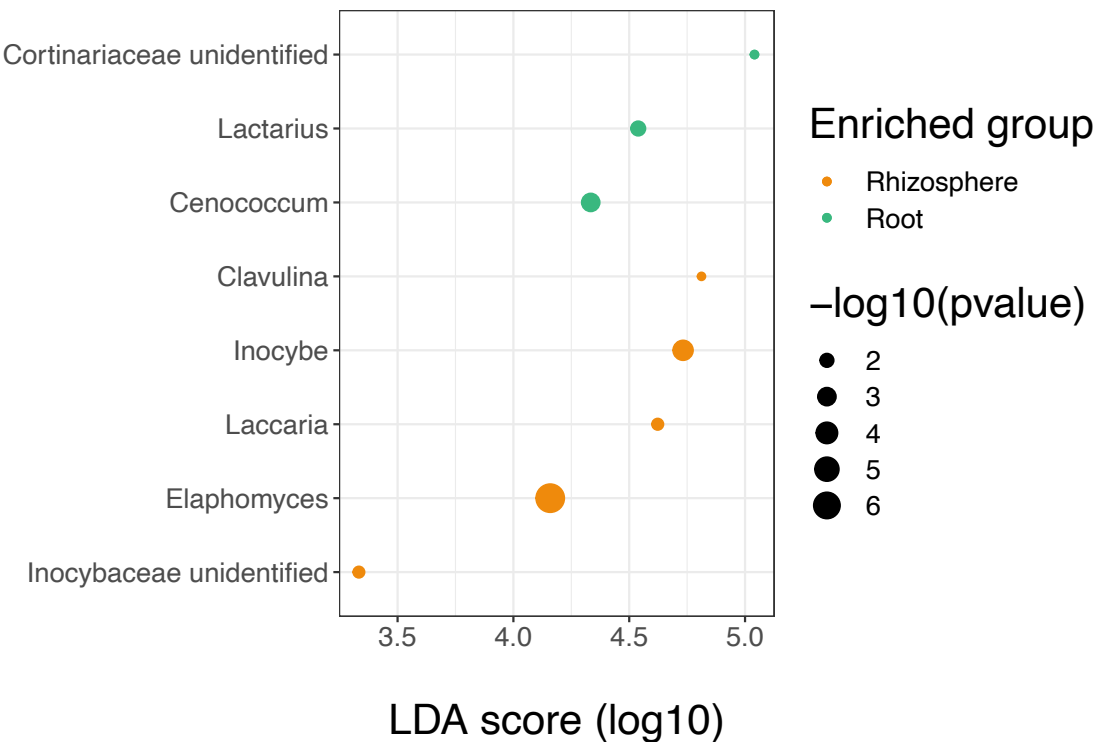
502 **Supplementary Figure 6: Root and rhizosphere have similar EcM community composition and**  
 503 **diversity.**

504 **(a)** EcM community composition of the rhizosphere and the roots of species collected in the F1 and F2  
 505 sites. **(b)** Shannon index of rhizosphere and root EcM community for the seven species collected in F1  
 506 and F2 sites. Different letters indicate significant differences in EcM diversity (post-hoc Tukey's test).



507  
 508

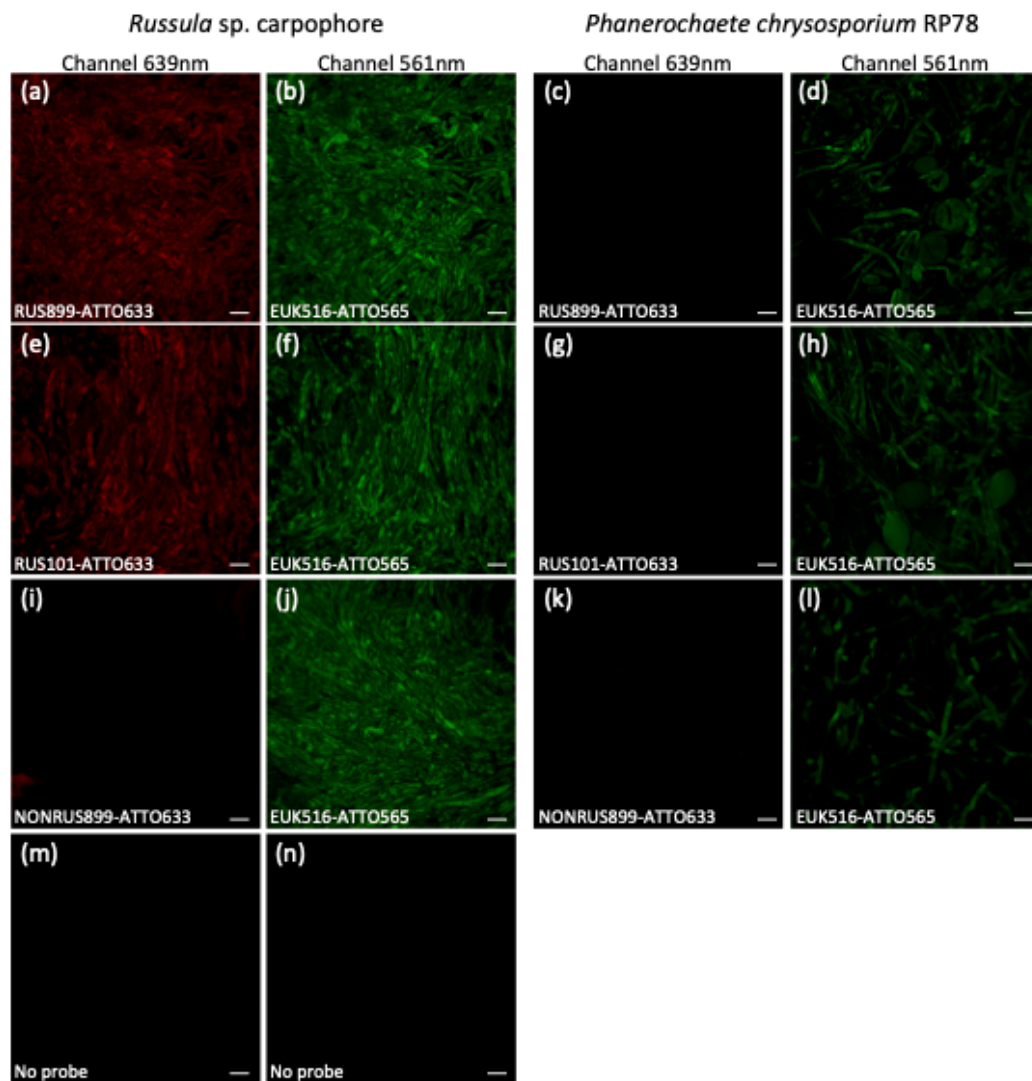
509 **Supplementary Figure 7: Some EcM genera are differentially abundant in roots and rhizosphere.**  
510 EcM genera significantly more abundant in roots or rhizosphere as computed using LEFsE procedure  
511 and their associated Linear Discriminant Analysis score (LDA; x-axis). The size of the dots corresponds  
512 to the log10 of the p-value computed by LEFsE.



513  
514

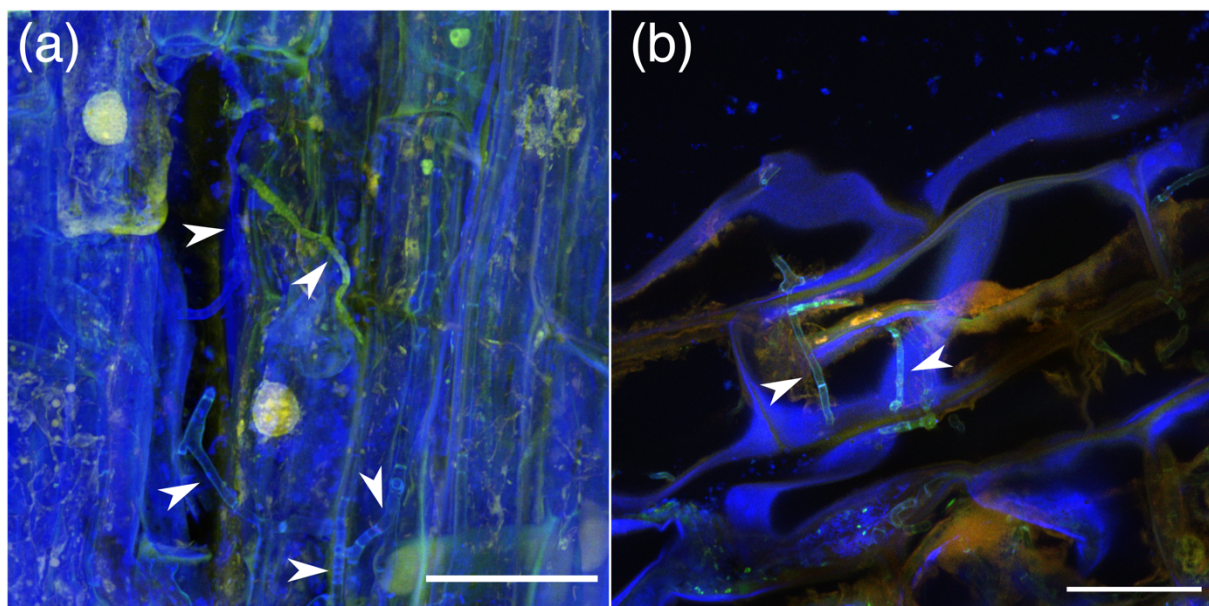
515 **Supplementary Figure 8: The newly designed probes Rus899 and Rus101 hybridize *in situ* with fungi**  
 516 **from the genus Russula.**

517 Evaluation of *FISH* probes targeting *Russula* 18S ribosomal RNA with ascocarps or cultivated hyphae  
 518 fixed from *Russula* sp. (left panel) or *Phanerochaete* sp. (right panel), respectively. Co-hybridization  
 519 experiments with (1) a non-specific probe targeting eukaryotic cells (EUK516, second column of each  
 520 panel) as a positive control with high signal intensity in the cytoplasm of fungal hyphae in combination  
 521 with (2) *Russula* probes; RUS899 (**a-b** and **c-d**) or RUS101 (**e-f** and **g-h**). For each co-detection, 2D  
 522 images obtained from each single channel are presented. Hybridization with *Russula* probes (RUS899  
 523 or RUS101) showed selective hybridization on *Russula* ascocarp with a good signal intensity in fungal  
 524 cytoplasm comparable to the positive probe EUK516, but not on hyphae from *Phanerochaete* culture.  
 525 Hybridization with a nonsense probe (NonRUS899, **i-j** and **k-l**) or with a hybridization buffer without  
 526 any *FISH* probe (**m** and **n**) demonstrates the absence of any fluorescence signal in the cytoplasm of  
 527 fungal hyphae. *Russula* sense and nonsense probes are coupled with ATTO633 dye and EUK516 is  
 528 coupled with ATTO565 dye. Identical laser power and gain detector were used for each image. Scale  
 529 bars: 10µm.



531 **Supplementary Figure 9: Observation of fungal hyphae in roots of *Carduus pycnocephalus* not**  
532 **hybridized with any FISH probe.**

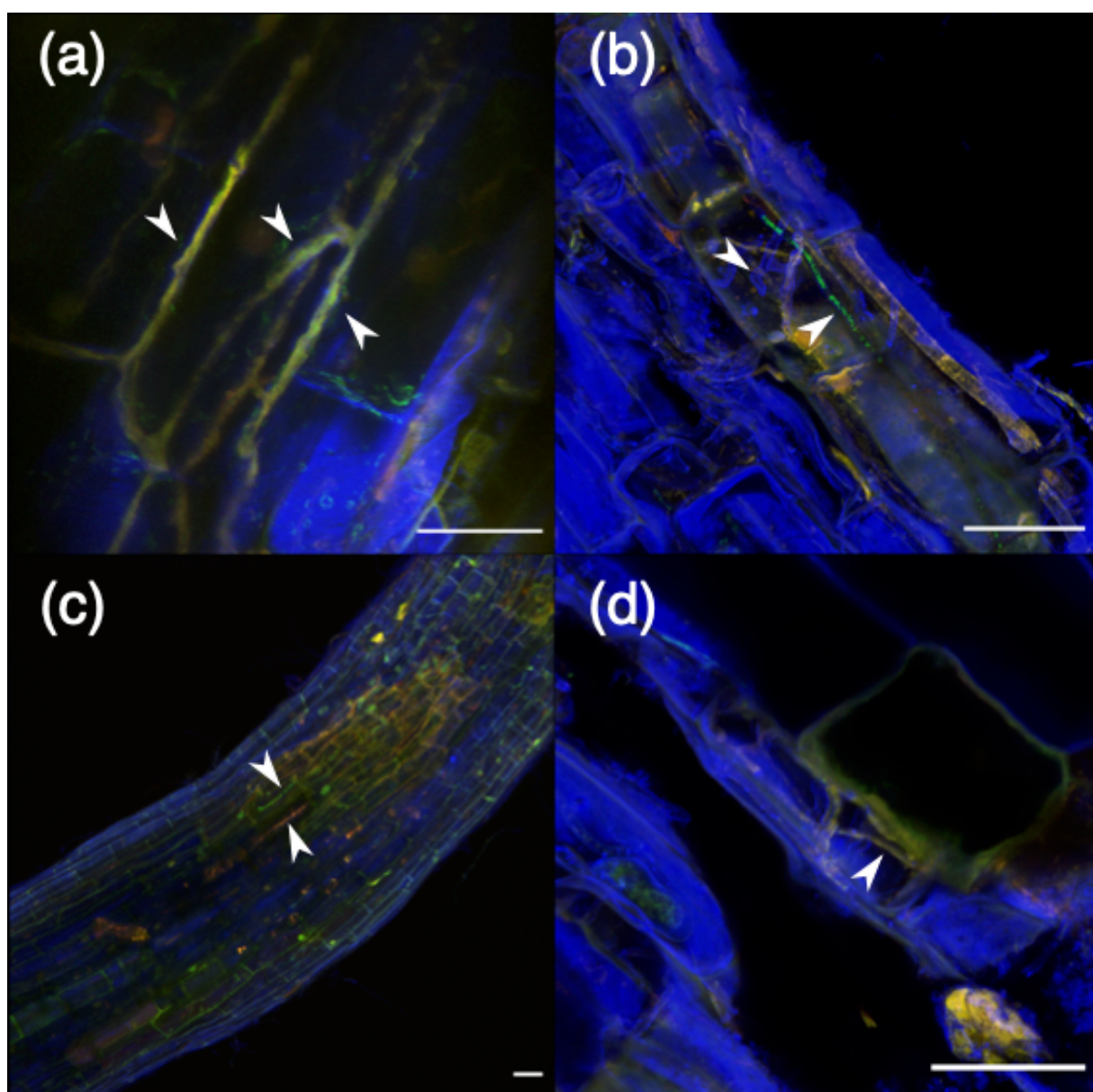
533 **(a), (b)** Negative controls to evaluate auto-fluorescence. Samples were processed with the same  
534 protocol of hybridization (Methods S4) but probes were replaced by sterile water (only the SR2000  
535 fluorescent dye was kept). Most of the hyphae observed had no cytoplasmic autofluorescence in the  
536 ranges of the generalist probe EUK516 (561 nm, green signal) and the *Russula* probes RUS899/101  
537 (639 nm, red signal), except in few cases where we could observe a fluorescent signal in the range of  
538 the EUK516 probe (green), as in (a). In (b), the red signal corresponds to plant tissues' autofluorescence  
539 at 639 nm. Scale bars: 30 µm.



540

541

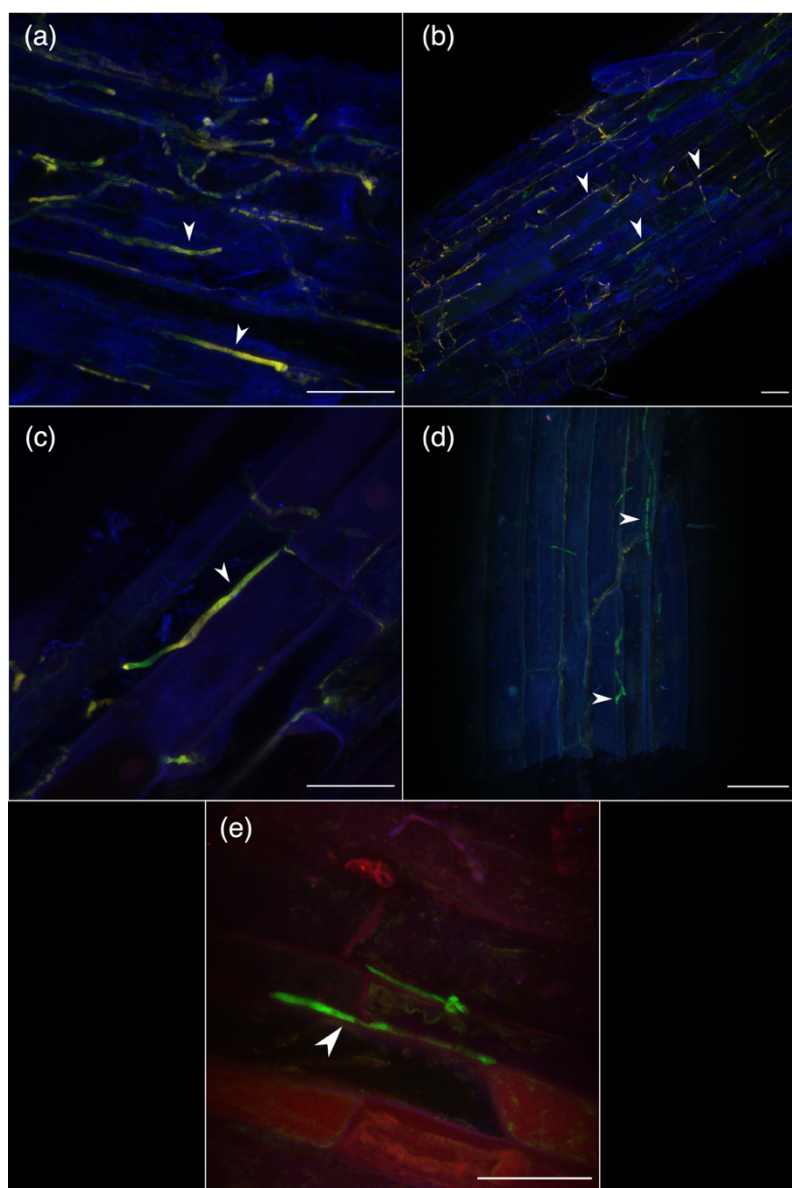
542 **Supplementary Figure 10: Observation of *Russula* spp. hyphae in the roots of *Carduus pycnocephalus***  
543 **and of hyphae of other fungal species with the sense and nonsense probes (controls).**  
544 (a), (c) Roots of *C. pycnocephalus* harboring *Russula* sp. hyphae co-hybridized with the *Russula*-specific  
545 probe RUS101-ATTO633 (red signal) and with the generalist probe EUK516-ATTO565 (green signal).  
546 Co-hybridization appears in yellow/orange. (a) Co-hybridized hyphae in the apoplast of plant cells. (c)  
547 Fungal hyphae only hybridized with the generalist probe (green; top arrow) and *Russula* sp. co-  
548 hybridized hyphae (bottom arrow). (b), (d) Nonsense controls: roots of *C. pycnocephalus* hybridized  
549 with the nonsense *Russula* probe NonRUS899-ATTO633 and the generalist probe EUK516-565. (b) We  
550 detected hyphae hybridized with the generalist probe (green signal, bottom arrow) and not hybridized  
551 at all (blue signal, top arrow). (d) Autofluorescence in the red spectrum was sometimes observed  
552 (green signal from the generalist probe + red autofluorescence; white arrow). Scale bars: 30 µm.



554 **Supplementary Figure 11: Observation of *Russula* spp. hyphae in the roots of *Ranunculus bulbosus*  
555 and of hyphae of other fungal species with the sense and nonsense probes (controls).**

556 **(a), (b)** Roots of *R. bulbosus* harboring *Russula* sp. hyphae hybridized with the *Russula*-specific probe  
557 RUS899-ATTO633 (red) and with the generalist probe EUK516-565 (green). Co-hybridization therefore  
558 appears yellow. **(c)** Roots of *R. bulbosus* harboring *Russula* sp. hyphae hybridized with the *Russula*-  
559 specific probe RUS101-ATTO633 (red) and with the generalist probe EUK516-565 (green). Co-  
560 hybridization therefore appears yellow. **(d)** Roots of *R. bulbosus* harboring a fungal hypha hybridized  
561 with the EUK516-565 (green) probe but not with the *Russula*-specific probe RUS101-ATTO633 (red).  
562 **(e)** Nonsense control: fungal hyphae in the roots of *R. bulbosus* hybridized with the nonsense *Russula*  
563 probe NonRUS899-ATTO633 (red signal) and the generalist probe EUK516-565 (green signal). Hyphae  
564 do not display any red signal (NonRUS899-ATTO633), showing that there is no unspecific binding from  
565 the probe. The red signal corresponds to plant cell wall autofluorescence. Scale bar: 30 µm.

566



567

## 568 References

- 569  
570 **Amann RI, Binder BJ, Olson RJ, Chisholm SW, Devereux R, Stahl DA.** 1990. Combination of 16S  
571 rRNA-targeted oligonucleotide probes with flow cytometry for analyzing mixed microbial  
572 populations. *Applied and Environmental Microbiology* **56**: 1919–1925.  
573 **Bahram M, Harend H, Tedersoo L.** 2014. Network perspectives of ectomycorrhizal associations.  
574 *Fungal Ecology* **7**: 70–77.  
575 **Bascompte J, Jordano P, Melián CJ, Olesen JM.** 2003. The nested assembly of plant–animal  
576 mutualistic networks. *Proceedings of the National Academy of Sciences* **100**: 9383–9387.  
577 **Blüthgen N, Menzel F, Blüthgen N.** 2006. Measuring specialization in species interaction networks.  
578 *BMC Ecology* **6**: 9.  
579 **Chagnon P-L, Bradley RL, Klironomos JN.** 2012. Using ecological network theory to evaluate the  
580 causes and consequences of arbuscular mycorrhizal community structure. *New Phytologist*  
581 **194**: 307–312.  
582 **Di Battista C, Selosse M-A, Bouchard D, Stenström E, Le Tacon F.** 1996. Variations in symbiotic  
583 efficiency, phenotypic characters and ploidy level among different isolates of the  
584 ectomycorrhizal basidiomycete *Laccaria bicolor* strain S 238. *Mycological Research* **100**:  
585 1315–1324.  
586 **Dormann CF, Fründ J, Schaefer HM.** 2017. Identifying Causes of Patterns in Ecological Networks:  
587 Opportunities and Limitations. *Annual Review of Ecology, Evolution, and Systematics* **48**:  
588 559–584.  
589 **Dormann CF, Gruber B, Fründ J.** 2008. Introducing the bipartite package: analysing ecological  
590 networks. *interaction* **1**: 8–11.  
591 **Dormann CF, Strauss R.** 2014. A method for detecting modules in quantitative bipartite networks.  
592 *Methods in Ecology and Evolution* **5**: 90–98.  
593 **Fernandes AD, Macklaim JM, Linn TG, Reid G, Gloor GB.** 2013. ANOVA-Like Differential Expression  
594 (ALDEx) Analysis for Mixed Population RNA-Seq. *PLOS ONE* **8**: e67019.  
595 **Garcia K, Delaux P-M, Cope KR, Ané J-M.** 2015. Molecular signals required for the establishment and  
596 maintenance of ectomycorrhizal symbioses. *New Phytologist* **208**: 79–87.  
597 **Gloor GB, Macklaim JM, Pawlowsky-Glahn V, Egoscue JJ.** 2017. Microbiome Datasets Are  
598 Compositional: And This Is Not Optional. *Frontiers in Microbiology* **8**.  
599 **van der Heijden MGA, Martin FM, Selosse M-A, Sanders IR.** 2015. Mycorrhizal ecology and  
600 evolution: the past, the present, and the future. *New Phytologist* **205**: 1406–1423.  
601 **Kivlin SN, Mann MA, Lynn JS, Kazenel MR, Taylor DL, Rudgers JA.** 2022. Grass species identity  
602 shapes communities of root and leaf fungi more than elevation. *ISME Communications* **2**: 1–  
603 11.  
604 **Legendre P, Gallagher ED.** 2001. Ecologically meaningful transformations for ordination of species  
605 data. *Oecologia* **129**: 271–280.  
606 **Lin H, Peddada SD.** 2020. Analysis of compositions of microbiomes with bias correction. *Nature  
607 Communications* **11**: 3514.  
608 **Martin F, Kohler A, Murat C, Veneault-Fourrey C, Hibbett DS.** 2016. Unearthing the roots of  
609 ectomycorrhizal symbioses. *Nature Reviews Microbiology* **14**: 760–773.  
610 **Martos F, Munoz F, Pailler T, Kottke I, Gonneau C, Selosse M-A.** 2012. The role of epiphytism in  
611 architecture and evolutionary constraint within mycorrhizal networks of tropical orchids.  
612 *Molecular Ecology* **21**: 5098–5109.  
613 **McKnight DT, Huerlimann R, Bower DS, Schwarzkopf L, Alford RA, Zenger KR.** 2019. Methods for  
614 normalizing microbiome data: An ecological perspective. *Methods in Ecology and Evolution*  
615 **10**: 389–400.  
616 **Montesinos-Navarro A, Segarra-Moragues JG, Valiente-Banuet A, Verdú M.** 2012. The network  
617 structure of plant–arbuscular mycorrhizal fungi. *New Phytologist* **194**: 536–547.  
618 **Nearing JT, Douglas GM, Hayes MG, MacDonald J, Desai DK, Allward N, Jones CMA, Wright RJ,  
619 Dhanani AS, Comeau AM, et al.** 2022. Microbiome differential abundance methods produce

- 620 different results across 38 datasets. *Nature Communications* **13**: 342.
- 621 **Nguyen NH, Song Z, Bates ST, Branco S, Tedersoo L, Menke J, Schilling JS, Kennedy PG. 2016.**
- 622 FUNGuild: An open annotation tool for parsing fungal community datasets by ecological
- 623 guild. *Fungal Ecology* **20**: 241–248.
- 624 **Nilsson RH, Larsson K-H, Taylor AFS, Bengtsson-Palme J, Jeppesen TS, Schigel D, Kennedy P, Picard**
- 625 **K, Glöckner FO, Tedersoo L, et al. 2019.** The UNITE database for molecular identification of
- 626 fungi: handling dark taxa and parallel taxonomic classifications. *Nucleic Acids Research* **47**:
- 627 D259–D264.
- 628 **Oksanen J, Blanchet FG, Kindt R, Legendre P, Minchin PR, O'hara RB, Simpson GL, Solymos P,**
- 629 **Stevens MHH, Wagner H. 2013.** Package ‘vegan’. *Community ecology package, version 2*: 1–
- 630 295.
- 631 **Olesen JM, Bascompte J, Dupont YL, Jordano P. 2007.** The modularity of pollination networks.
- 632 *Proceedings of the National Academy of Sciences* **104**: 19891–19896.
- 633 **Op De Beeck M, Lievens B, Busschaert P, Declerck S, Vangronsveld J, Colpaert JV. 2014.** Comparison
- 634 and Validation of Some ITS Primer Pairs Useful for Fungal Metabarcoding Studies (B Neilan,
- 635 Ed.). *PLoS ONE* **9**: e97629.
- 636 **Peay KG, Bruns TD, Kennedy PG, Bergemann SE, Garbelotto M. 2007.** A strong species-area
- 637 relationship for eukaryotic soil microbes: island size matters for ectomycorrhizal fungi.
- 638 *Ecology Letters* **10**: 470–480.
- 639 **Perez-Lamarque B, Petrolli R, Strullu-Derrien C, Strasberg D, Morlon H, Selosse M-A, Martos F.**
- 640 **2022.** Structure and specialization of mycorrhizal networks in phylogenetically diverse
- 641 tropical communities. *Environmental Microbiome* **17**: 38.
- 642 **Petrolli R, Zinger L, Perez-Lamarque B, Collobert G, Griveau C, Pailler T, Selosse M-A, Martos F.**
- 643 **2022.** Spatial turnover of fungi and partner choice shape mycorrhizal networks in epiphytic
- 644 orchids. *Journal of Ecology* **110**: 2568–2584.
- 645 **Pichon B, Goff RL, Morlon H, Perez-Lamarque B. 2023.** Telling mutualistic and antagonistic ecological
- 646 networks apart by learning their multiscale structure. : 2023.04.04.535603.
- 647 **Plett JM, Daguerre Y, Wittulsky S, Vayssières A, Deveau A, Melton SJ, Kohler A, Morrell-Falvey JL,**
- 648 **Brun A, Veneault-Fourrey C, et al. 2014.** Effector MiSSP7 of the mutualistic fungus *Laccaria*
- 649 bicolor stabilizes the *Populus* JAZ6 protein and represses jasmonic acid (JA) responsive genes.
- 650 *Proceedings of the National Academy of Sciences* **111**: 8299–8304.
- 651 **Pölme S, Bahram M, Jacquemyn H, Kennedy P, Kohout P, Moora M, Oja J, Öpik M, Pecoraro L,**
- 652 **Tedersoo L. 2018.** Host preference and network properties in biotrophic plant-fungal
- 653 associations. *New Phytologist* **217**: 1230–1239.
- 654 **Rognes T, Flouri T, Nichols B, Quince C, Mahé F. 2016.** VSEARCH: a versatile open source tool for
- 655 metagenomics. *PeerJ* **4**: e2584.
- 656 **Roy-Bolduc A, Laliberté E, Hijri M. 2016.** High richness of ectomycorrhizal fungi and low host
- 657 specificity in a coastal sand dune ecosystem revealed by network analysis. *Ecology and*
- 658 *Evolution* **6**: 349–362.
- 659 **Schneider-Maunoury L, Deveau A, Moreno M, Todesco F, Belmondo S, Murat C, Courty P, Jąkalski**
- 660 **M, Selosse M. 2020.** Two ectomycorrhizal truffles, *Tuber melanosporum* and *T. aestivum*,
- 661 endophytically colonise roots of non-ectomycorrhizal plants in natural environments. *New*
- 662 *Phytologist* **225**: 2542–2556.
- 663 **Schneider-Maunoury L, Leclercq S, Clément C, Covès H, Lambourdière J, Sauve M, Richard F,**
- 664 **Selosse M-A, Taschen E. 2018.** Is *Tuber melanosporum* colonizing the roots of herbaceous,
- 665 non-ectomycorrhizal plants? *Fungal Ecology* **31**: 59–68.
- 666 **Segata N, Izard J, Waldron L, Gevers D, Miropolsky L, Garrett WS, Huttenhower C. 2011.**
- 667 Metagenomic biomarker discovery and explanation. *Genome Biology* **12**: R60.
- 668 **Selosse M-A, Dubois M-P, Alvarez N. 2009.** Do Sebacinales commonly associate with plant roots as
- 669 endophytes? *Mycological Research* **113**: 1062–1069.
- 670 **Selosse M-A, Petrolli R, Mujica MI, Laurent L, Perez-Lamarque B, Figura T, Bourceret A, Jacquemyn**
- 671 **H, Li T, Gao J, et al. 2021.** The Waiting Room Hypothesis revisited by orchids: were orchid

- 672 mycorrhizal fungi recruited among root endophytes? *Annals of Botany*: mcab134.
- 673 **Susana Rivera C, Eugenia Venturini M, Oria R, Blanco D. 2011.** Selection of a decontamination
- 674 treatment for fresh *Tuber aestivum* and *Tuber melanosporum* truffles packaged in modified
- 675 atmospheres. *FOOD CONTROL* **22**: 626–632.
- 676 **Toju H, Guimarães PR, Olesen JM, Thompson JN. 2014.** Assembly of complex plant–fungus
- 677 networks. *Nature Communications* **5**: 5273.
- 678 **Toju H, Tanabe AS, Ishii HS. 2016.** Ericaceous plant–fungus network in a harsh alpine–subalpine
- 679 environment. *Molecular Ecology* **25**: 3242–3257.
- 680 **Untergasser A, Cutcutache I, Koressaar T, Ye J, Faircloth BC, Remm M, Rozen SG. 2012.** Primer3—
- 681 new capabilities and interfaces. *Nucleic Acids Research* **40**: e115.
- 682 **Uroz S, Courty PE, Oger P. 2019.** Plant Symbionts Are Engineers of the Plant-Associated Microbiome.
- 683 *Trends in Plant Science* **24**: 905–916.
- 684 **Waud M, Busschaert P, Ruyters S, Jacquemyn H, Lievens B. 2014.** Impact of primer choice on
- 685 characterization of orchid mycorrhizal communities using 454 pyrosequencing. *Molecular*
- 686 *Ecology Resources* **14**: 679–699.
- 687 **White TJ, Bruns T, Lee S, Taylor J. 1990.** AMPLIFICATION AND DIRECT SEQUENCING OF FUNGAL
- 688 RIBOSOMAL RNA GENES FOR PHYLOGENETICS. In: PCR Protocols. Elsevier, 315–322.
- 689